NUREG/IA–0175
NSI RRC KI90–12/1–3–00
IPSN/00–13

International Agreement Report

Analysis of Pin-by-Pin Effects for LWR Rod Ejection Accident

Prepared by
A. Avvakumov, V. Malofeev, V. Sidorov

Nuclear Safety Institute
Russian Research Centre
"Kurchatov Institute"
Kurchatov Square 1
Moscow 123182
Russia

Office of Nuclear Regulatory Research
U.S. Nuclear Regulatory Commission
Washington, DC 20555–0001

March 2000

Prepared for
U.S. Nuclear Regulatory Commission, Institute for Protection and Nuclear Safety (France),
and Ministry of Science and Technologies of the Russian Federation

Published by
U.S. Nuclear Regulatory Commission

AVAILABILITY NOTICE

Availability of Reference Materials Cited in NRC Publications

NRC publications in the NUREG series, NRC regulations, and *Title 10, Energy,* of the *Code of Federal Regulations,* may be purchased from one of the following sources:

1. The Superintendent of Documents
   U.S. Government Printing Office
   P.O. Box 37082
   Washington, DC 20402–9328
   <http://www.access.gpo.gov/su_docs>
   202–512–1800
2. The National Technical Information Service
   Springfield, VA 22161–0002
   <http://www.ntis.gov>
   1–800–553–6847 or locally 703–605–6000

The NUREG series comprises (1) brochures (NUREG/BR-XXXX), (2) proceedings of conferences (NUREG/CP-XXXX), (3) reports resulting from international agreements (NUREG/IA-XXXX), (4) technical and administrative reports and books [(NUREG-XXXX) or (NUREG/CR-XXXX)], and (5) compilations of legal decisions and orders of the Commission and Atomic and Safety Licensing Boards and of Office Directors' decisions under Section 2.206 of NRC's regulations (NUREG-XXXX).

A single copy of each NRC draft report for comment is available free, to the extent of supply, upon written request as follows:

Address: Office of the Chief Information Officer
Reproduction and Distribution
Services Section
U.S. Nuclear Regulatory Commission
Washington, DC 20555–0001
E–mail: <DISTRIBUTION@nrc.gov>
Facsimile: 301–415–2289

A portion of NRC regulatory and technical information is available at NRC's World Wide Web site:

<http://www.nrc.gov>

After January 1, 2000, the public may electronically access NUREG-series publications and other NRC records in NRC's Agencywide Document Access and Management System (ADAMS), through the Public Electronic Reading Room (PERR), link <http://www.nrc.gov/NRC/ADAMS/index.html>.

Publicly released documents include, to name a few, NUREG-series reports; *Federal Register* notices; applicant, licensee, and vendor documents and correspondence; NRC correspondence and internal memoranda; bulletins and information notices; inspection and investigation reports; licensee event reports; and Commission papers and their attachments.

Documents available from public and special technical libraries include all open literature items, such as books, journal articles, and transactions, *Federal Register* notices, Federal and State legislation, and congressional reports. Such documents as theses, dissertations, foreign reports and translations, and non-NRC conference proceedings may be purchased from their sponsoring organization.

Copies of industry codes and standards used in a substantive manner in the NRC regulatory process are maintained at the NRC Library, Two White Flint North, 11545 Rockville Pike, Rockville, MD 20852–2738. These standards are available in the library for reference use by the public. Codes and standards are usually copyrighted and may be purchased from the originating organization or, if they are American National Standards, from—

American National Standards Institute
11 West 42nd Street
New York, NY 10036–8002
<http://www.ansi.org>
212–642–4900

NUREG/IA-0175
NSI RRC KI90-12/1-3-00
IPSN/00-13

International Agreement Report

Analysis of Pin-by-Pin Effects for LWR Rod Ejection Accident

Prepared by
A. Avvakumov, V. Malofeev, V. Sidorov

Nuclear Safety Institute
Russian Research Centre
"Kurchatov Institute"
Kurchatov Square 1
Moscow 123182
Russia

Office of Nuclear Regulatory Research
U.S. Nuclear Regulatory Commission
Washington, DC 20555-0001

March 2000

Prepared for
U.S. Nuclear Regulatory Commission, Institute for Protection and Nuclear Safety (France),
and Ministry of Science and Technologies of the Russian Federation

Published by
U.S. Nuclear Regulatory Commission

ABSTRACT

This study was undertaken to demonstrate capabilities of the pin-by-pin model used by the BARS code and to understand various effects of intra-assembly pin-by-pin representation of fuel power, burnup and temperature in calculational analysis of light water reactor rod ejection accidents (LWR REAs). Effects of pin-by-pin fuel power and burnup representation were investigated on the basis of calculations for the peripheral control rod ejection in VVER-1000 of the South Ukrainian NPP Unit 1. Comparative analysis of the REA in pressurized water reactor (PWR) of Three Mile Island Unit 1 using the BARS code with the diffusion nodal codes PARCS and CRONOS2 was done. The important differences in obtained results and effects of pin-by-pin fuel temperature representation are discussed in the report.

TABLE OF CONTENTS

LIST OF FIGURES

LIST OF TABLES

ACKNOWLEDGMENTS

The authors would like to thank Drs. V. Asmolov (RRC KI, Russia) who was the initiator and coordinator of this work, R. O. Meyer, D. D. Ebert (US NRC) and J. Papin (IPSN, France) for their supervision and support of this project.

The authors pay a high tribute to untimely deceased Dr. Franz Schmitz for his special contribution into this project.

The authors would also like to acknowledge the contributions of Drs. S. Pylev (RRC KI, Russia) who assisted during the coupling of the neutronic and thermal-hydraulic models, A. Dukhovensky (RRC KI, Russia) who provided the data on VVERs, A. Aronson (BNL, USA), T. J. Downar and H. G. Joo (Purdue University, USA) who provided the input deck for PWR calculations.

Special acknowledgement is given to Dr. D. J. Diamond (BNL, USA) for his many suggestions and comments during this work.

Finally, the authors wish to thank Mr. G. Abyshov for his help in preparing the final report.

1. INTRODUCTION

Large deformations of the power distribution in the core accompany the course of certain reactivity initiated accidents (RIAs) such as rod ejection (REA), steam line break and boron dilution in a pressurized water reactor (PWR). At present 3 D best-estimate neutronic models are widely used for the analysis of these accidents instead of very conservative 1 D – 2 D methodologies. Best-estimate methods are available to calculate maximum fuel pellet enthalpy that expresses acceptance criteria for RIAs, but it is important to determine the uncertainty in the calculated fuel enthalpy.

Practically in all modern best-estimate neutronic codes the fuel assembly is represented as homogenized region (an assembly-by-assembly approach). As indicated in Reference 1 such a code could underestimate fuel enthalpy for the rod drop accident in a boiling water reactor by approximately 100%. The main sources of the underestimation in the calculated fuel enthalpy for this accident were an uncertainty in control rod worth and an systematic error due to intra-assembly power peaking. If the code calculates only an assembly averaged power distribution the latter error could be considerable. To eliminate this systematic error methods for a pin-by-pin reconstruction of the power distribution within the assembly are begun to apply in dynamic calculations. However, the reconstruction approaches require a special validation for transients. In this manner one of the important problem is to understand whether it is necessary to take into account feedbacks due to detailed intra-assembly power distribution.

Since a best-estimate dynamic code is meant to calculate events that have not been observed in actual plants a comparison with other codes is made to validate one for the events of interest. However, the comparison for codes of the similar neutronic nature (the assembly-by-assembly diffusion approach) does not allow to clarify understanding the uncertainty in the calculated results for a number of the key parameters. To improve this understanding the comparison should be done with the qualitatively different code with more rigorous neutronic model.

Recently in Russian Research Centre "Kurchatov Institute" a plant dynamic model for VVER and PWR RIA calculation has been developed. The model is based on the coupling of the RELAP5/MOD3.2 thermal hydraulic code with the BARS 3 D detailed neutronic code and is intended to calculate a wide range of RIAs in light water reactors (LWRs) including control rod ejection, boron dilution and steam line break (Refs. 2, 3, and 4). The BARS code performs the reactor calculation in framework of full-scale pin-by-pin neutronic model with an explicit representation of each fuel pin (up to 80,000 calculational cells). This model is based on an advanced method of heterogeneous reactor theory that is more rigorous than widely used homogeneous diffusion approach and is appropriated to direct pin-by-pin calculations.

In previous studies a validation of the heterogeneous method for LWRs was made for large variety of calculational and experimental benchmarks (Refs. 4-7). It was shown that the BARS code predicts multiplication factor (K_{eff}) and pin-by-pin power distribution in complicated configurations of the critical assembly not worse than precise Monte Carlo and transport codes. It was also demonstrated the RELAP-BARS code capabilities for VVER REA modeling.

The main objective of this study was to assess the effect of a detailed intra-assembly representation of the power, fuel temperature, and burnup on the course of LWR REAs. An analysis of this effect allows to improve the understanding of the uncertainty in best-estimate REA calculations.

The effect of the pin-by-pin power representation was demonstrated by the RELAP-BARS calculation of the VVER-1000 REA and by comparison of the RELAP-BARS results with the PARCS and CRONOS2 best-estimate calculations for the TMI-1 PWR REA benchmark (Refs. 8-10). To analyze the effect of the fuel rod temperature non-uniformity a special method for pin-by-pin fuel temperature reconstruction was developed and validated. The effect was assessed for the TMI-1 PWR REA benchmark. To analyze the effect of the detailed fuel burnup representation a 3 D pin-by-pin fuel cycle model was developed and validated. The assessment of this effect was made for the VVER-1000 REA.

Section 2 expounds features of the heterogeneous method. Section 3 contains a review of the validation results of the heterogeneous model for LWR pin-by-pin neutronic calculations. The results include a validation of reactivity coefficients, a pin-by-pin power distribution, and a power pulse transient. Section 4 focuses on the RELAP-BARS LWR plant dynamic model. It also consists in a description of the method for the intra-assembly reconstruction of the pin-by-pin fuel temperature distribution. Section 5 describes the BARS pin-by-pin fuel cycle model. Section 6 contains the validation results for the VVER-1000 pin-by-pin calculations of fuel burnup and fuel cycle. Section 7 assesses the effect of the pin-by-pin fuel power and burnup representation on the course of the VVER-1000 REA. Section 8 analyzes the effect of a detailed intra-assembly representation of the power and fuel temperature on the course of the TMI-1 PWR REA. The conclusions are drawn concerning the importance of the pin-by-pin representations.

2. ADVANCED HETEROGENEOUS METHOD FOR LWR PIN-BY-PIN CALCULATIONS

The BARS code was developed on the basis of the advanced method of heterogeneous reactor theory. The heterogeneous method is based on analytical representation of the neutron flux distribution in the form of Green's functions superposition. For LWR applications this method allows directly to take into account detailed structure of the core by explicit representation of fuel pins, absorber rods, etc. The Green's function is derived from a solution of a few group diffusion equation for an infinite uniform media with a singular source at the cell axis. The intensities of the singular sources are determined in such a way that relationship between neutron flux and current at the boundary of each reactor cell coincides with that obtained from the precise transport calculation of a single cell. The latter relationship is defined by means of a boundary condition matrix (Λ-matrix). This matrix is determined as a result of a set of neutron transport calculations for the cell with varying neutron currents at the cell boundary (Ref. 11). In comparison with few group neutron cross sections Λ-matrices provide for the same accuracy of the reactor calculation by smaller number of energy groups.

An axial dependence of the neutron flux is found by Fourier series expansion. As a result of the solution of the original differential equations, a set of linear algebraic equations is obtained. These general heterogeneous equations connect all pairs of the reactor cells. It leads to unresolved computation problem in reactor calculations because the reactors with only small number of cells could be calculated by using even modern computers. To produce equations to connect only neighboring cells a difference approximation of the Green's functions is performed (Ref. 12).

To calculate fast transients, the heterogeneous method uses "time absorption" matrices instead of the traditional neutron velocities (Ref. 3). The spatial-time neutron flux distribution within a time step is represented in a form of a product of a time-dependent amplitude function and a spatial-dependent form-function (quasi-static approach). The amplitude function is determined by solving point kinetic equations. Parameters of the reactor point kinetics are found using a perturbation

theory method. The form-function is determined by solving linear equations system with a delayed neutron source. To reduce the number of 3 D calculations during the transient a special term describing the reactivity dependence due to reactor energy release feedback is included into the point kinetic equations.

It should be noted that the heterogeneous theory does not require the validity of the diffusion approximation over the reactor. The diffusion equations are used only to determine Green's function shape that weakly influences the reactor calculation accuracy. It is very important for pin-by-pin calculation of LWRs with heterogeneous structure of modern fuel assemblies. It should be also noted that unlike a homogenized assembly LWR calculation a pin-by-pin one requires a rather large number of energy groups because of a small size of cells. As the BARS validation results showed, Λ-matrix approach allows to make pin-by-pin LWR calculations with reasonable accuracy using only 4-5 groups.

The neutron data base of BARS (Λ-matrices) is calculated by the TRIFON code (Ref. 11). TRIFON solves the multigroup neutron transport equation in various reactor cells using the collision probability method taking into account detailed structure of resonant cross sections. Strong resonances are calculated explicitly by an additional division of the basic energy mesh within the resonance. Weak resonances are taken into account approximately in framework of the effective resonance level model (Ref. 13). This approach allowed to reduce significantly a required total number of groups.

The neutron database of TRIFON was generated by the NJOY code on the basis of ENDF/B-VI library (Refs. 14 and 15). The TRIFON basic energy mesh consists of 89 groups (24 in fast neutron region and 65 in thermal one). The major resonance of ^{234}U, ^{236}U, ^{240}Pu, ^{242}Pu and 11 most strong resonances of ^{238}U are calculated explicitly. The resonances of ^{238}U above 210 eV are calculated by 6 effective resonance levels. The total number of energy groups is about 350. This resonant treatment was validated by comparison with calculational results obtained by the UNK code, which uses very fine energy mesh with 7,000 energy groups (Refs. 16 and 5).

3. REVIEW OF VALIDATION RESULTS

To demonstrate the capability of the BARS pin-by-pin calculations to predict LWR neutronic parameters some results of previous studies are presented. These results refer to a validation of most important parameters – reactivity coefficients, a pin-by-pin power distribution, and a power pulse transient.

3.1. Reactivity Coefficients

Accuracy in prediction of the reactivity coefficients is a key factor in the analysis of LWR transients, especially for RIA conditions. To analyze uncertainties in prediction of the reactivity coefficients, a number of PWR and BWR benchmark fuel cells were calculated by the TRIFON code. All the benchmark calculations were performed using Monte Carlo codes MCNP-3A (with data library based on ENDF/B-V) and MCNP-4A (ENDF/B-VI) (Refs. 17-19).

Table 3.1 presents the calculational results for the Doppler coefficient in PWR fresh fuel cells as compared with Monte Carlo benchmark calculations for different fuel enrichment (ε_f). Monte Carlo result is given with a single standard deviation (σ) from the mean as an uncertainty; ε is relative deviation in TRIFON result in comparison with MCNP-3A (ε_3) and MCNP-4A (ε_4). Comparison of the presented data shows that almost all the TRIFON results are in excellent agreement with the MCNP calculations.

Table 3.1 Calculational Results for the Doppler Coefficient in PWR Fresh Fuel Cells

ε_f (%)	MCNP-3A $\alpha_D \pm \sigma$	MCNP-4A $\alpha_D \pm \sigma$	TRIFON		
			α_D	ε_3 (%)	ε_4 (%)
0.7	- 5.429 ± 0.760	- 5.468 ± 0.323	- 5.52531	1.77	1.04
1.6	- 3.558 ± 0.310	- 3.388 ± 0.207	- 3.43951	- 3.34	1.51
2.4	- 2.715 ± 0.277	- 2.754 ± 0.157	- 2.82679	4.11	2.64
3.1	- 2.584 ± 0.225	- 2.789 ± 0.137	- 2.51830	- 2.53	- 9.69
3.9	- 2.370 ± 0.187	- 2.534 ± 0.155	- 2.40529	1.49	- 5.08

MCNP-4A (ENDF/B-VI) benchmark calculations for BWR fuel cells were carried out for a wide range of fuel enrichment, fuel and moderator temperatures, moderator void fraction and the fuel burnup. The total number of calculated fuel cells (except for cells with Gd) is 77. Tables 3.2 - 3.4 present a summary of the TRIFON calculational results for the Doppler coefficient, the void coefficient and the moderator temperature coefficient as compared with Monte Carlo calculations depending on fuel burnup.

Table 3.2 Calculational Results for the Doppler Coefficient in BWR Fuel Cells

Burnup (GWd/ST)	Nos. of calculations	Deviation from MCNP-4A (%)	
		Max	RMS
0	13	6.8	4.3
10	12	7.1	3.4
35	12	11.6	7.3

Table 3.3 Calculational Results for the Void Coefficient in BWR Fuel Cells

Burnup (GWd/ST)	Nos. of calculations	Deviation from MCNP-4A (%)	
		Max	RMS
0	6	2.0	1.1
10	6	2.2	1.3
35	6	3.5	2.2

Table 3.4 Calculational Results for the Moderator Temperature Coefficient in BWR Fuel Cells

Burnup (GWd/ST)	Nos. of calculations	Deviation from MCNP-4A (%)	
		Max	RMS
0	4	5.5	2.8
10	3	6.4	4.3
35	3	13.2	7.7

The results show the following. The TRIFON calculations of the Doppler coefficient give very good results for the fresh and slightly burnup fuel: the root mean square (RMS) deviation is 3-4 %; as for cells with fuel burnup of 35 GWd/ST this value is 7 % (this is quite satisfactory result). Calculational accuracy to predict the void effect is very high: the TRIFON and MCNP results are in agreement of no more than 4 %. As for the moderator temperature coefficient, almost all the TRIFON results are within 3σ of the MCNP results.

3.2. Pin-by-Pin Power Distribution

To validate the LWR pin-by-pin model, experimental results obtained at ZR-6 critical assembly were used (Ref. 20). These results include measurements of a water critical level and the pin-by-pin distribution of fuel activation. ZR-6 assembly consists of shortened VVER fuel rods with fuel enrichment of 1.6, 3.6, 4.4%, absorber rods of a different type and water cells. The moderator temperature was 20, 80 and 130°C. Boric acid concentration in the moderator was up to 8 g/l. The total number of critical configurations with a fuel lattice of 12.7 mm (lattice of VVER-1000 type) selected for a validation of the LWR pin-by-pin model is 107.

All assemblies may be divided into the following types according to their configurations:

- uniform configurations (single-zone and double-zone);
- Xn type configurations with absorbers or water holes in each n-th lattice position;
- K91 "fuel assembly" type configurations (19 "fuel assemblies", each having 91 cells);
- K271 "fuel assembly" type configurations (7 "fuel assemblies", each having 271 cells);
- K331 "fuel assembly" type configurations (1 "fuel assembly" with 331 cells).

All of the calculations were performed by using the BARS code with 5-group neutron data bases prepared by the TRIFON code with ENDF/B-VI.

In Figures 3.1 - 3.8 core loading patterns and a radial distribution of the fuel activation (both calculated and measured) are presented for some configurations. The calculated data were normalized to the mean value over experimental data. Radial distributions of the fuel activation are given in directions, pointed at the core loading pattern: experimental data - by symbols and calculated ones - by curves.

Table 3.5 presents the BARS calculational results for the multiplication factor and the calculational accuracy in prediction of the pin-by-pin fuel activation distribution. All data in Table 3.5 were averaged on each type of assemblies and for all assemblies. Each K_{eff} value is given together with the corresponding mean square deviation for the assemblies of this type. For a comparison corresponding results for the KENO-V Monte Carlo code and the HELIOS transport code are presented (Refs. 21 and 22).

Table 3.5 BARS Calculational Results for ZR-6 Assemblies

Code	Type of assembly	Nos. of assemblies	Mean value of K_{eff}	RMS (%)
BARS	Uniform	33	0.99494 ± 0.00165	1.33
BARS	Xn	39	0.99706 ± 0.00275	1.65
BARS	K91	11	0.99731 ± 0.00199	1.91
BARS	K271	12	0.99487 ± 0.00155	-
BARS	K331	12	0.99614 ± 0.00166	1.29
BARS	All types	107	0.99608 ± 0.00207	1.49
KENO-V	All types	107	0.99480 ± 0.00360	-
HELIOS	—	34	1.00244 ± 0.00368	1.44

The calculational results show that the BARS code with rather high accuracy predicts the multiplication factor and the spatial distribution of the fuel activation for the cores of a complex geometry with rather strong local deformations in the neutron flux due to various types of the perturbation (the water cells, the absorbers, the water gap or even the trap). It should be mentioned that the BARS calculational accuracy for ZR-6 assemblies is not worse in comparison with KENO-V and HELIOS for a precise calculation of fuel assemblies.

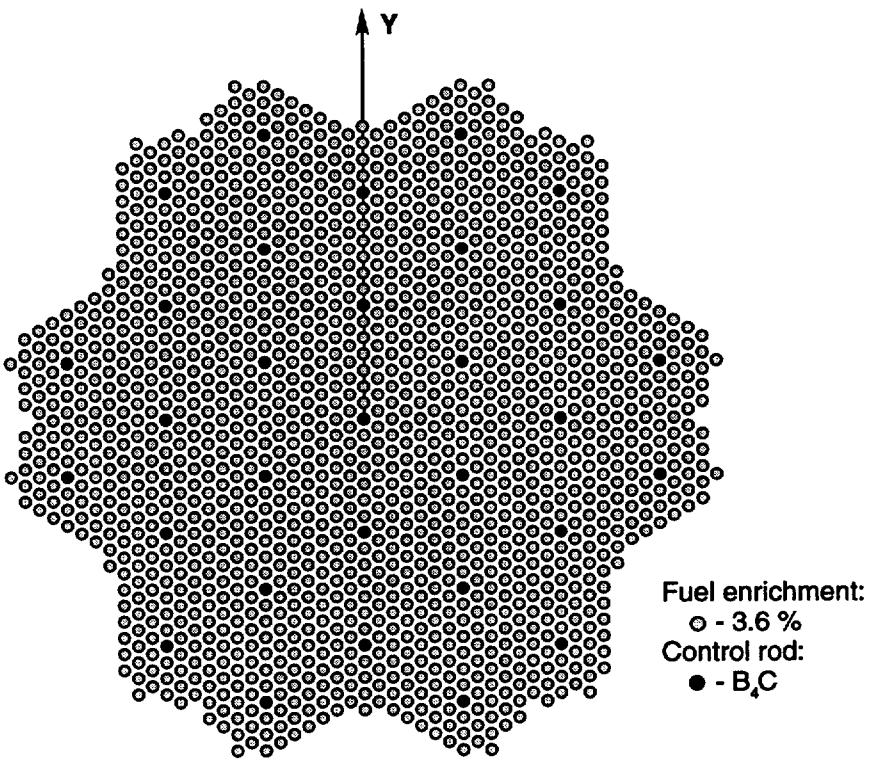

Figure 3.1 Critical Assembly ZR-6. Loading Pattern 244/244

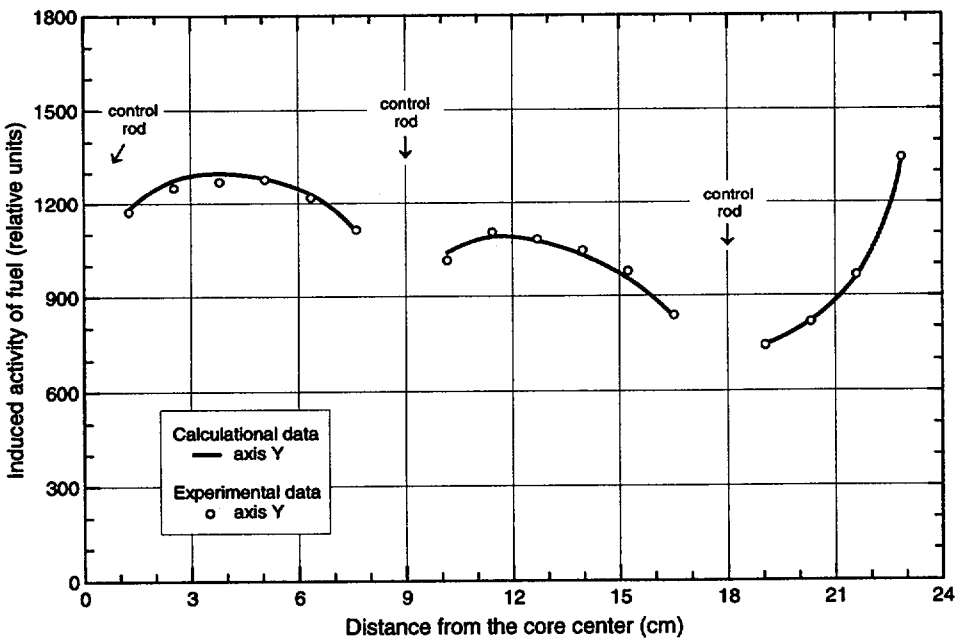

Figure 3.2 Comparison of Calculational and Experimental Data for Assembly 244/244

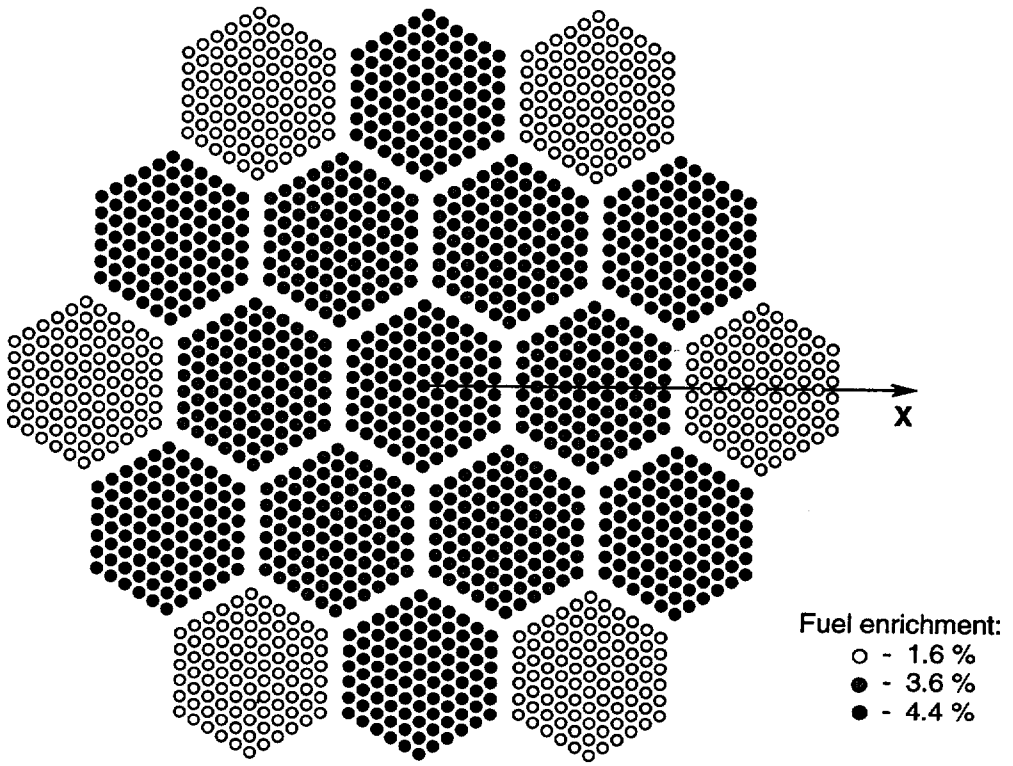

Figure 3.3 Critical Assembly ZR-6. Loading pattern 113/113

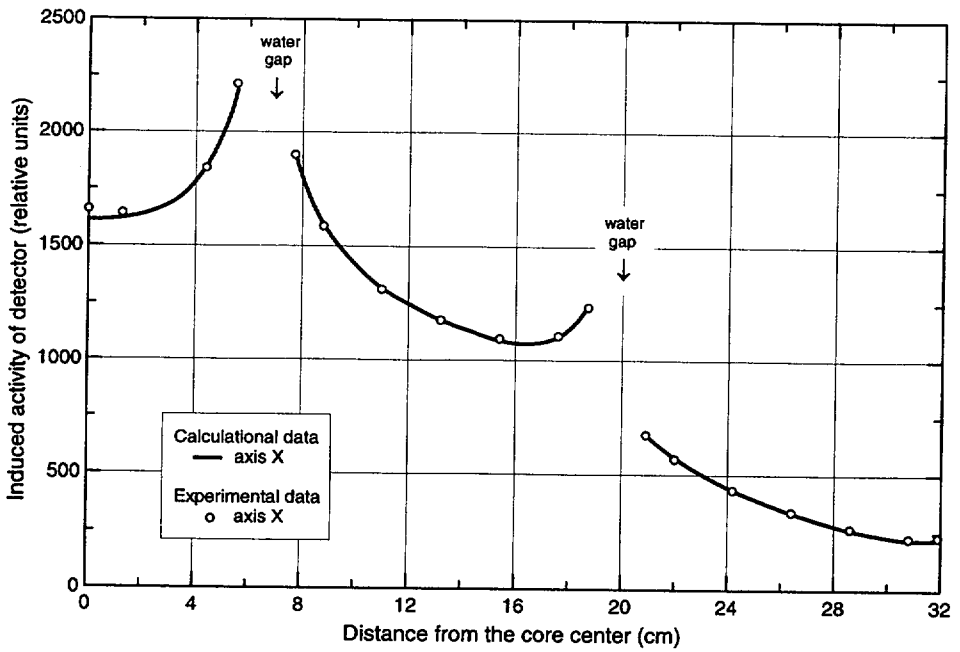

Figure 3.4 Comparison of Calculational and Experimental Data for Assembly 113/113

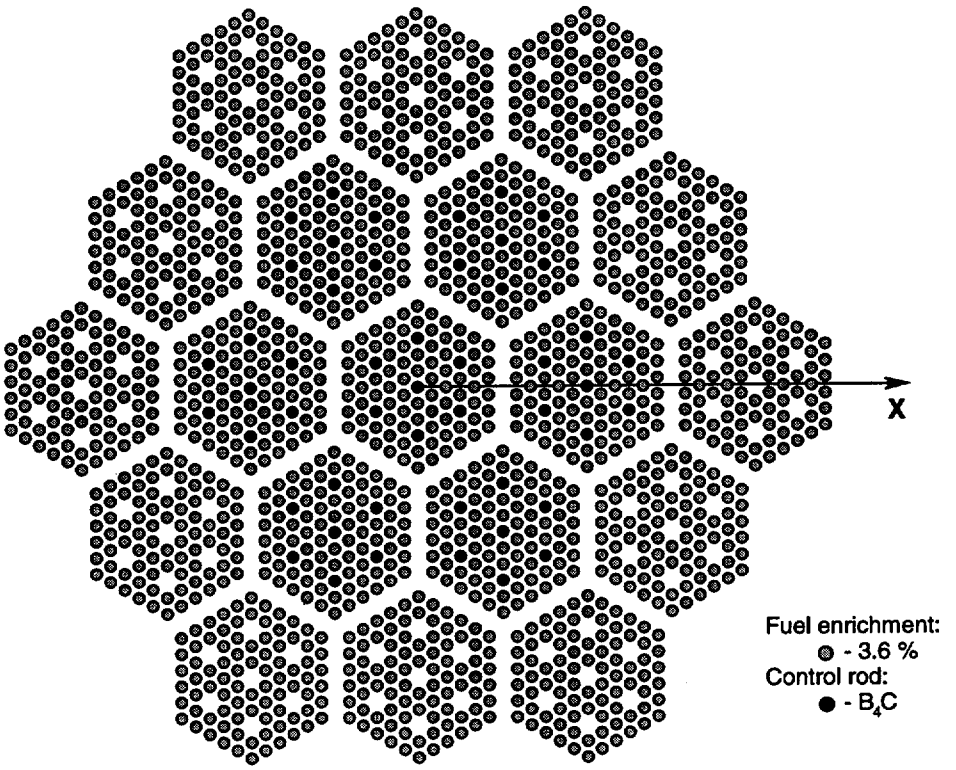

Figure 3.5 Critical Assembly ZR-6. Loading Pattern 103/103

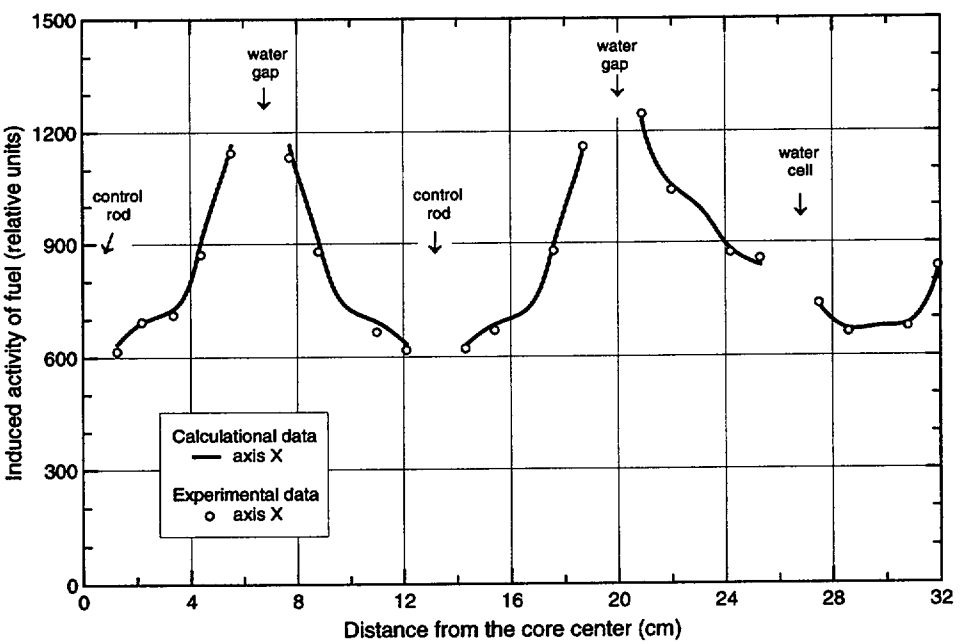

Figure 3.6 Comparison of Calculational and Experimental Data for Assembly 103/103

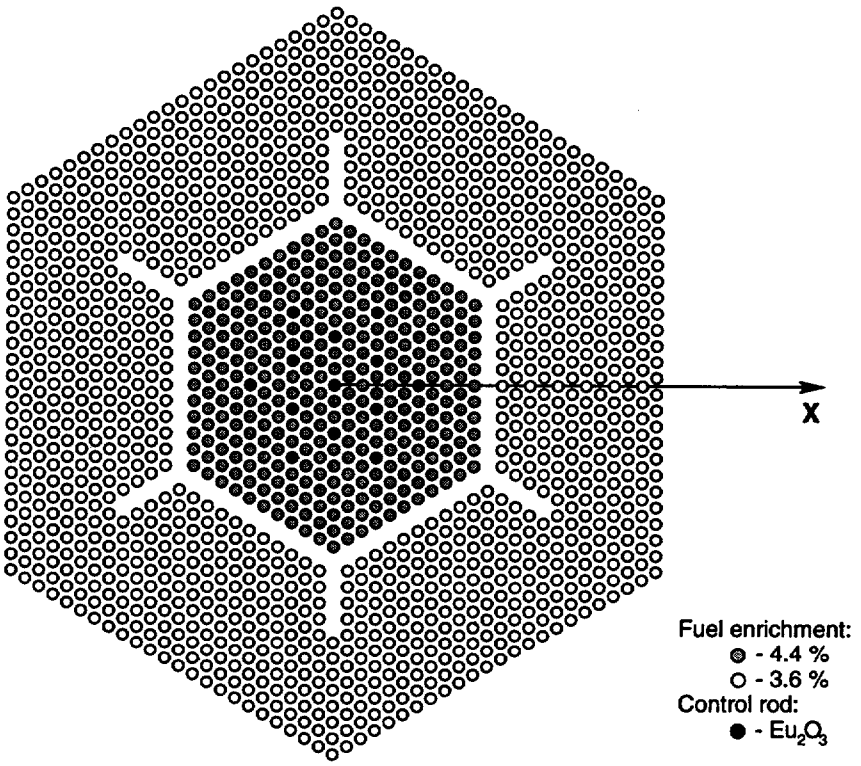

Figure 3.7 Critical Assembly ZR-6. Loading pattern 144/144

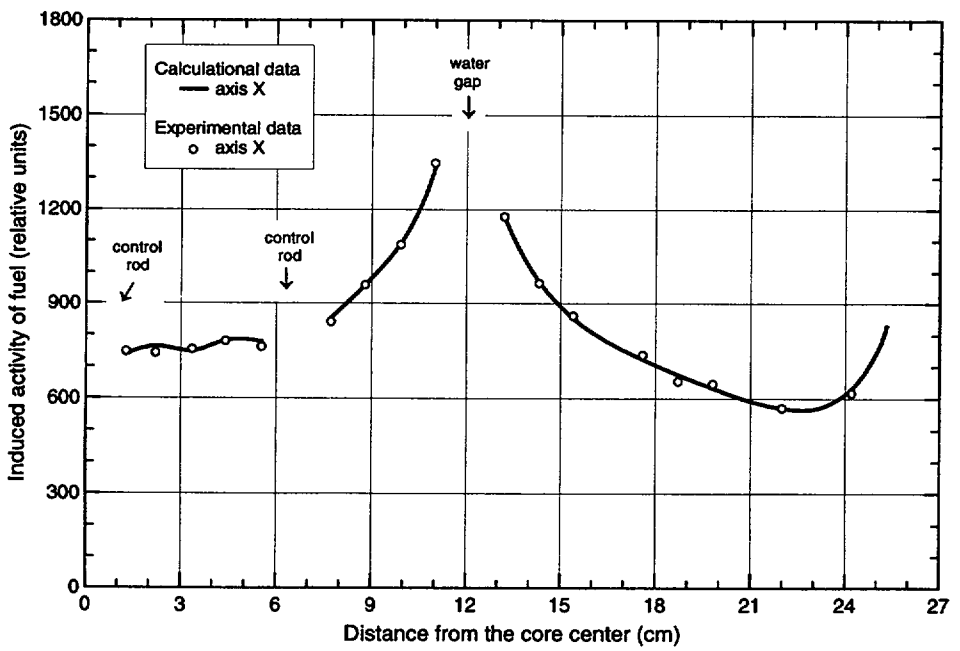

Figure 3.8 Comparison of Calculational and Experimental Data for Assembly 144/144

3.3. Power Pulse Transient

To validate the BARS pin-by-pin transient model, experimental results of the power dynamic behavior obtained at the pulsed graphite reactor IGR were used. IGR is intended to test reactor fuel rods under RIA conditions.

The basic feature of such transients is the fact that the power rise is initiated by a control rod withdrawal and is suppressed by the negative temperature feedback: the increase in the graphite temperature leads to the increase in the thermal neutron leakage and, as a result, to a large negative reactivity insertion. Such experiments that model the control rod ejection accident in LWR with temperature feedback are unknown.

The reactor core (see Figure 3.9) consists of graphite columns impregnated with highly enriched uranium. In the core center there is a central experimental channel where the capsule containing test fuel rod samples is to be loaded. The core is surrounded by a graphite reflector, a thermal shield and a water tank. To control reactor operations 16 Gd rods in the core and in the reflector are used. The time dependence of the reactor power was measured by means of a set of out-core ionization chambers in the water tank and in-core detectors located near the experimental capsule.

The dynamic behavior of IGR in pulse experiments is characterized by: sharp changes in the reactor power; significant deformations of the neutron flux; strong heterogeneity in the core graphite temperature distribution; effects of the control rod interference and the graphite heating up on the control rod worth; a strong dependence of the prompt neutron lifetime and the feedback coefficient on the reactor core temperature.

The validation of the BARS transient module was performed on the basis of experiments carried out at IGR with inserted reactivity within 0.9 - 1.8 β (β - delayed neutron fraction). The IGR power time profile was recorded by 6 ionization chambers and 3 in-core detectors. Figure 3.10 shows the comparison of the calculational and

experimental results for the test with inserted reactivity of 1.8 β. As shown in the figure, calculated and measured power time profiles are in an excellent agreement.

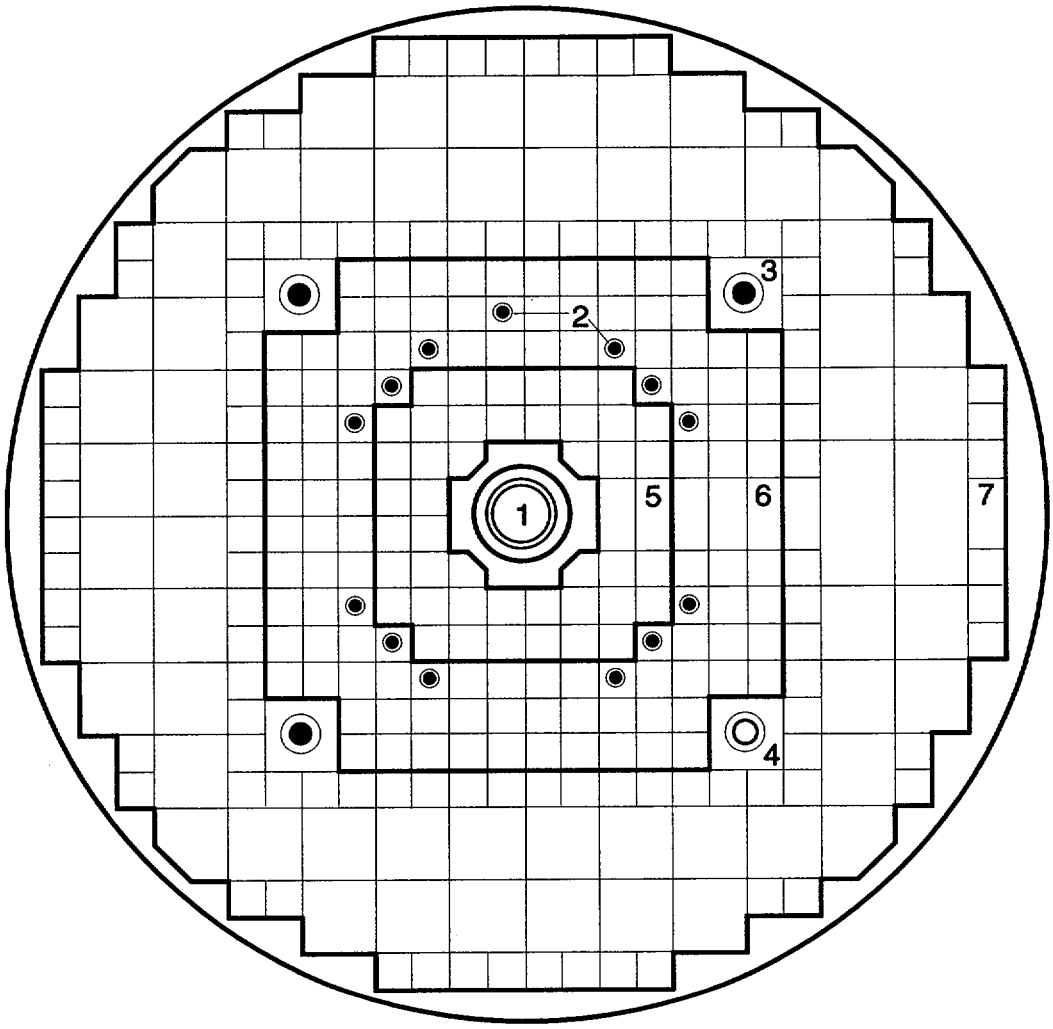

1 - central experimental channel;
2 - control rod channel;
3 - shim rod channel;
4 - lateral experimental channel;
5 - internal part of the core;
6 - external part of the core;
7 - graphite reflector.

Figure 3.9 Cross-Sectional Layout of IGR Reactor

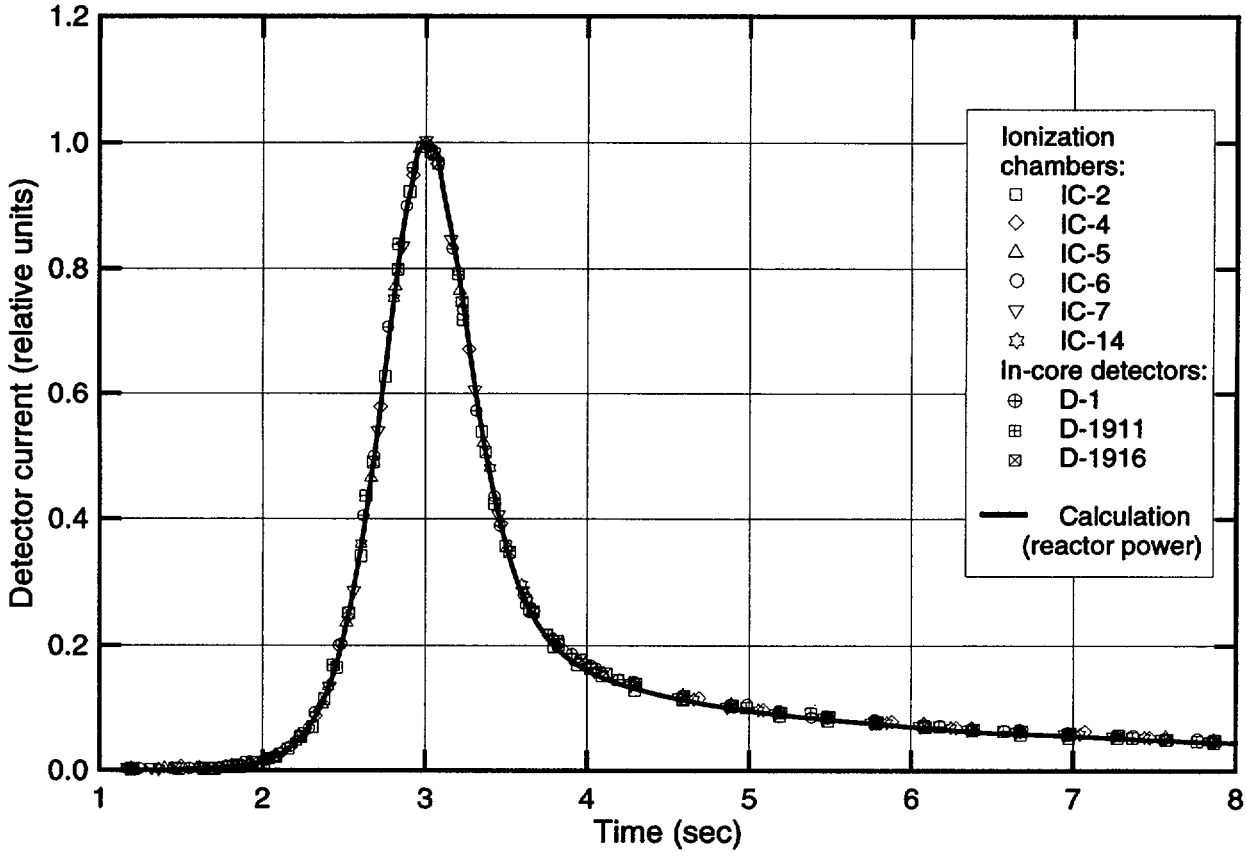

Figure 3.10 Comparison of Calculational and Experimental Data for the Pulse with Inserted Reactivity of 1.8 β at IGR Reactor.

4. RELAP - BARS PLANT DYNAMIC MODEL

4.1. Description of the Coupled Model

A specific feature of the RELAP - BARS coupling is a large computational cost per one time step of the BARS code in comparison with RELAP5/MOD3 code. Mentioned above feature of the BARS kinetic method allows to choose time step for whole reactor calculations depending only on degree of variations in power shape, in spite of variations in total reactor power, thermal hydraulic parameters and feedbacks. In virtue of it, the BARS time step, as a rule, is much larger than the RELAP one, with the exception of time periods of a fast reactivity insertion (a control rod ejection). For this reason, the neutronic calculation in each time step is divided into the following stages:

1. The calculation of the neutron flux spatial-energy form-function and the delayed neutron precursor distributions. It requires the largest computational time.
2. The calculation of point kinetic parameters, the amplitude function and the determination of the pin-by-pin power distribution. This stage requires a much smaller computational time compared with a single step calculation by RELAP.

The first stage calculations are performed rather seldom depending on the reactor power distribution changes. The second stage calculations are carried out at each time step determined by RELAP.

The RELAP-BARS coupling is based on certain options of the RELAP5/MOD3 code that allows to tabulate the reactor power distribution as a function of spatial coordinates and time, and to connect an additional subroutine to the RELAP code. In the framework of the RELAP model, the BARS neutronic calculation can be considered as determination of the core power distribution as a function of spatial coordinates and time for the RELAP next time step taking into account thermal hydraulic feedbacks. In this case the BARS code can be considered as a subroutine of the RELAP code, while preserving the logic of thermal hydraulic calculations.

To provide the data exchange between the RELAP and BARS codes, the COTT interface code is used. This code calculates also pin-by-pin fuel temperature distribution by the reconstruction method and some additional thermal hydraulic parameters, which are not calculated by RELAP. Besides, the COTT code contains simplified thermal hydraulic option based on 1 D single- or two-phase homogeneous flow with a slip ration. This option is used for thermal-hydraulic calculation of the core during slow transients such as fuel cycle modeling.

The reconstruction procedure is described below.

Before the transient modeling, the plant initial steady state is calculated. The neutronic calculation of the reactor steady state is performed by the BARS steady-state option, which solves the non-linear eigenvalue problem. During the coupled neutronic - thermal hydraulic calculation the core initial conditions can be automatically adjusted.

The following adjustment possibilities are available:

- to change the neutron generation rate,
- to change the axial position of some control rods or control rod banks,
- to change the boric acid concentration in the coolant.

Unlike the dynamic calculation of the plant initial steady-state, the adjusted steady-state calculation allows rather quickly to balance neutronic and thermal hydraulic processes without a variation in the reactor power.

The plant initial steady-state calculation by the RELAP - BARS code is performed in two stages:

- the RELAP steady-state calculation without using the BARS code at a predetermined reactor power,
- the iterative calculation of the plant steady-state by the RELAP - BARS code.

Then the dynamic calculation is performed. The transient neutronic calculation is carried out by the BARS time-dependent option, and the thermal hydraulic calculation - by the RELAP dynamic option. Figure 4.1 shows the scheme of the sequence of the RELAP - BARS calculations.

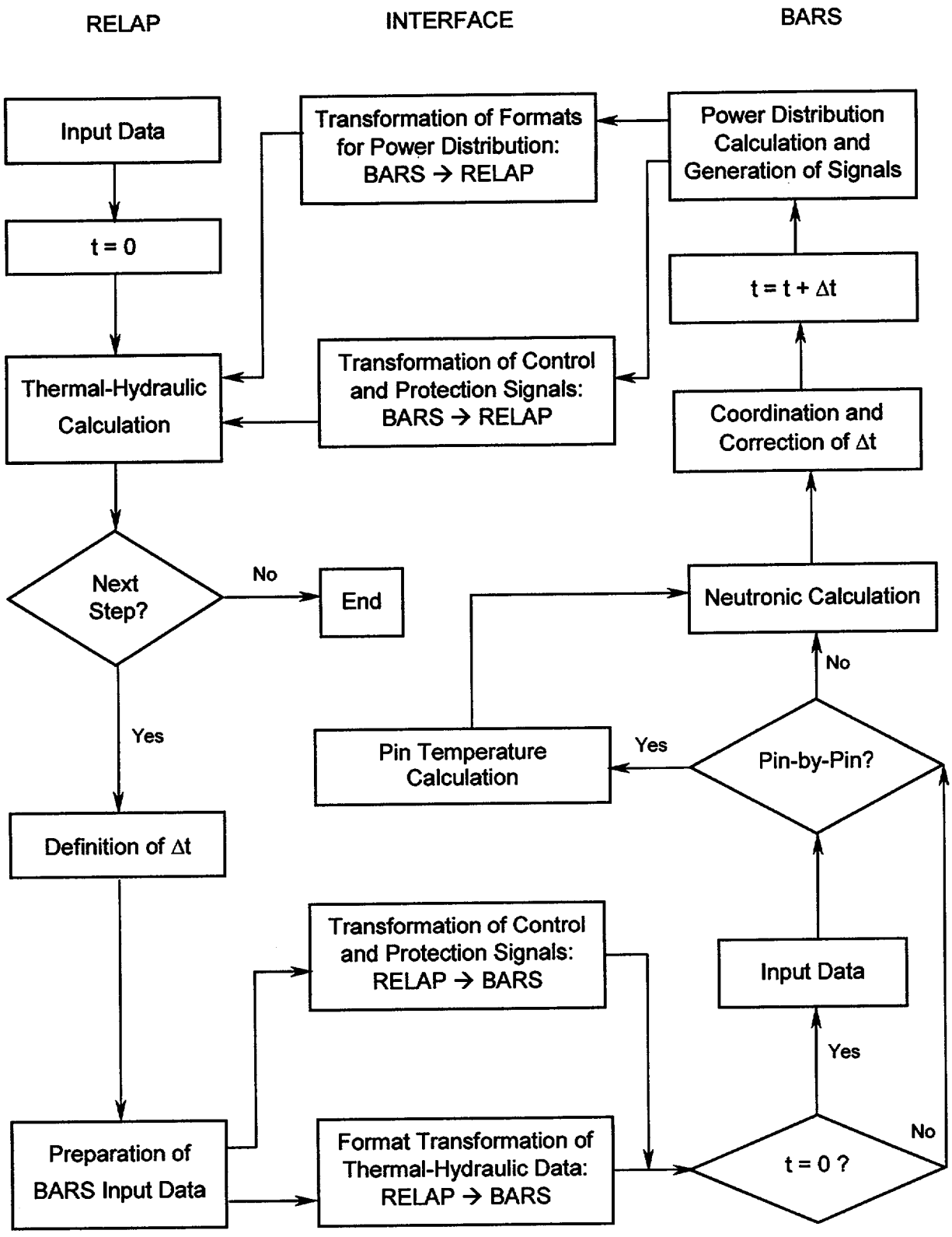

Figure 4.1 Scheme of RELAP – BARS Coupling

4.2. Reconstruction of the Pin-by-Pin Fuel Temperature Distribution

In practice the RELAP5/MOD3.2 code could not be used for full-scale pin-by-pin core thermal hydraulic calculations because of the input deck restriction and an extremely large running time. That is why a new method to reconstruct a 3 D pin-by-pin fuel temperature distribution was developed. Since a number of the hottest fuel pins can be calculated by RELAP directly, the pin-by-pin fuel temperature representation is needed only to take into account the effect of the intra-assembly fuel temperature distribution on the Doppler feedback, and since this effect is not expected to be large, a very high accuracy for the pin-by-pin fuel temperature reconstruction is not required. From the other side the reconstruction procedure has to be a fast-running one because of total number of the fuel pins within the LWR core is typically about 50,000. Therefore, the reconstruction method that leads to a simple analytical expression for the fuel temperature was proposed.

The method is based on a representation of the radial averaged fuel rod temperature for any axial node by sum of two terms:

$$T_k(t) = T(t) + \theta_k(t)$$

where

$T_k(t)$ is the radial averaged fuel rod temperature,

$T(t)$ is the radial averaged fuel temperature for the rod with averaged power, calculated by RELAP,

$\theta_k(t)$ is the deviation of the radial averaged fuel rod temperature from T,

k is the index of the rod within the fuel assembly.

To obtain the expression for $\theta_k(t)$, the following approximations are used:

- the heat transfer coefficient, the coolant temperature, and the fuel and cladding volumetric heat capacities and conductivities are identical for all rods within the assembly;
- the fuel thermal conductivity and volumetric heat capacity are determined by T;

- a radial dependence of the deviation of the fuel rod temperature from the fuel temperature for the rod with averaged power, calculated by RELAP, is described by a parabola;
- a radial dependence of the deviation of the cladding temperature from the cladding temperature for the rod with averaged power is linear.

Within any RELAP time step these approximations allow to formulate the linear Fourier equations for the radial dependence of the fuel and cladding temperature deviations. Integrating and summing these equations over the radial direction, the heat balance equation for the rod is obtained. It contains a heat flux at the cladding surface. To exclude the heat flux from the heat balance equation, the boundary condition at the cladding surface and the approximations for the fuel and cladding temperature deviations are used. As a result the following equation for $\theta_k(t)$ is obtained:

$$c\, d\theta_k(t)/dt = q_k - (2/r)\, \alpha\, \theta_k(t)\,, \quad t_{j-1} \le t \le t_j$$

with the initial condition

$$\theta_k(t_0) = \theta^0_k$$

where

c is the fuel volumetric heat capacity,

$$q_k = Q_k(t) - Q(t),$$

$Q_k(t)$ is the fuel rod volumetric heat source,

Q(t) is the assembly average volumetric heat source,

r is the fuel pellet radius,

j is the RELAP time step index,

$$1/\alpha = 1/\alpha_f + 1/\alpha_g + 1/\alpha_c + 1/\alpha_l,$$

α_f is the fuel thermal conductivity,

α_g is the gas gap thermal conductivity,

α_c is the cladding thermal conductivity,

α_l is the cladding - coolant thermal conductivity.

This differential equation has a simple analytical solution that can be given for any RELAP time step with index "j" as below:

$$\theta_k(t_j) = (q_k/\alpha)\,(1 - \exp(-\alpha/c\Delta t_j) + \theta_k(t_{j-1})\exp(-\alpha/c\Delta t_j)), \quad \Delta t_j = t_j - t_{j-1}.$$

Thus, the determination of the pin-by-pin fuel temperature distribution consists of two stages:

- an assembly-by-assembly fuel temperature calculation by the RELAP code using an assembly averaged power distribution, calculated by the BARS code;
- pin-by-pin fuel temperature reconstruction within each assembly by the COTT code used as an interface code between RELAP and BARS.

5. BARS PIN-BY-PIN FUEL CYCLE MODEL

The solution of a problem of modeling of a LWR fuel cycle concerns a wide spectrum of neutronic and thermal-hydraulic phenomena taking place in the reactor core and other plant systems. To take into account all of these phenomena in details is rather problematic, but the pin-by-pin approach allows modeling the fuel cycle in more realistic manner.

The main goal in such a calculation is to predict a fuel nuclide composition as a function of the cycle time. Fuel cycle codes, based on an assembly-by-assembly representation of the core, used consequently assembly averaged fuel burnup. Such approximation may lead to an uncertainty in safety analysis of the high burnup core.

In this Section, the BARS pin-by-pin fuel cycle model is briefly described from the point of view of its advantages compared with an assembly-by-assembly method.

The pin-by-pin approach used in BARS allows, in principle, to create a fuel cycle model in which fuel depletion equations could be solved directly for each calculational node according to neutronic and thermal-hydraulic parameters calculated for this node. A database of such a "direct" model will include Λ-matrices for each node recalculated by the TRIFON code after the routine BARS calculational step. The reasons why this model was not realized were as follows:

- number of the calculational nodes is 1,000,000 (50,000 pins $\times$ 20 axial layers);
- the TRIFON running time to calculate 1 node is about 10-12 s.

Thus, a total time to generate the database for a single burnup step is equal to about 120 days. That is why a fuel cycle model with the database calculated in advance (instead of "direct" calculations during the cycle) has been developed.

The fuel cycle model implemented in the BARS code is based on the following approaches:

- calculation of a fuel nuclide composition and generation of the database;
- calculation of the fuel cycle with the precalculated database.

Figure 5.1 gives a schematic structure of the BARS fuel cycle model.

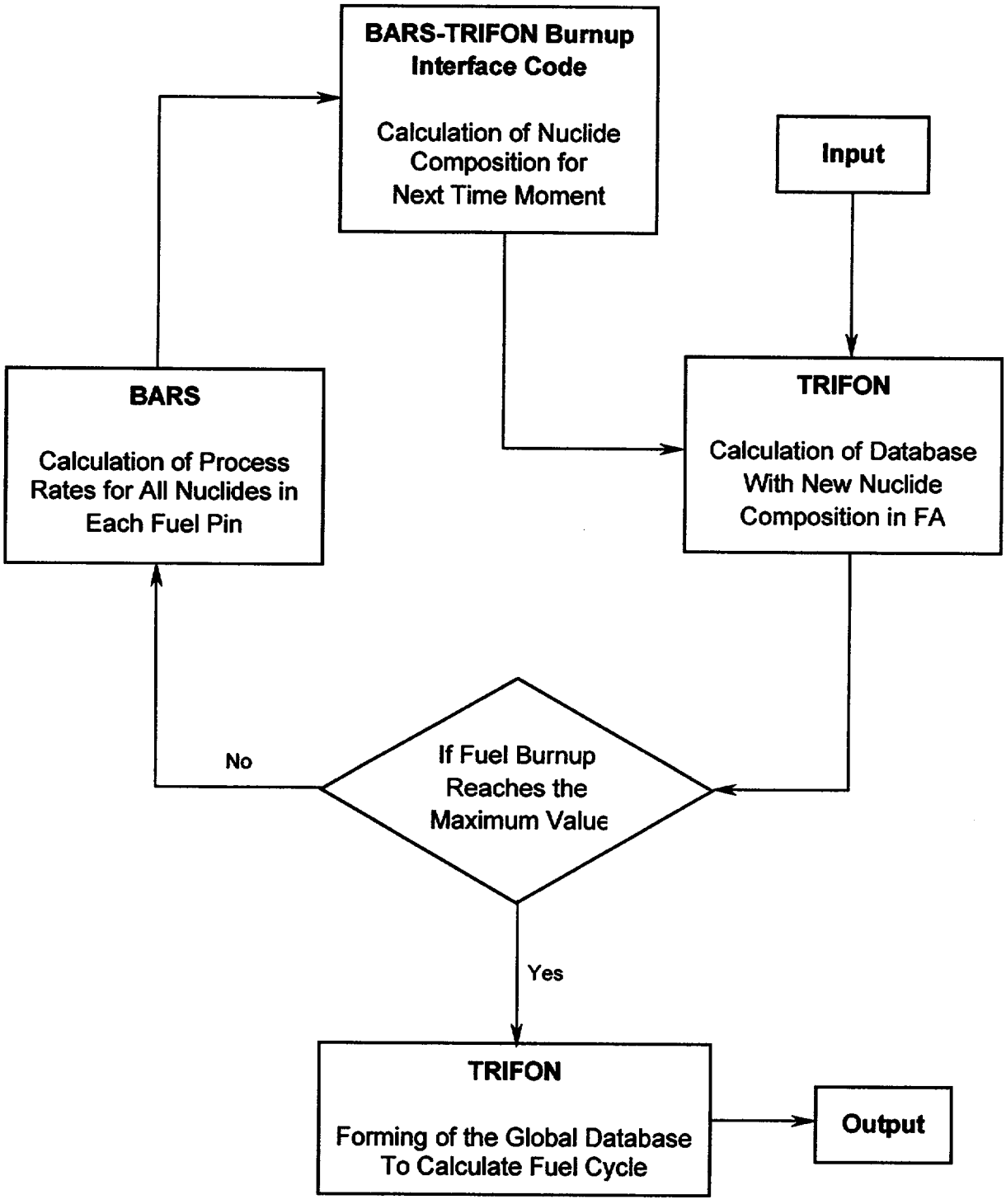

Figure 5.1 Structure of the BARS Fuel Cycle Model

5.1. Calculation of Fuel Nuclide Composition and Database Generation

This stage may be considered as two independent steps.

The first step includes calculation of the nuclide composition in fuel rods within a single fuel assembly calculated by the BARS code. The criticality is kept up by varying the neutron current at the assembly outer boundary. Initial database for the BARS code is calculated by the TRIFON code for the fresh fuel. For each fuel rod the BARS code calculates neutron absorption and generation rates which are used as coefficients in a set of depletion equations solved by a special interface routine. This interface code uses nuclide transformation scheme taking into account 24 heavy nuclides, 49 explicit fission products and 4 lumped fission products (Reference 23). Fuel rods nuclide compositions determined at each burnup step are used as input data for the TRIFON code for the next recalculation of the BARS database. Calculations are carried out at fixed thermal-hydraulic parameters with given dependencies of power and boron concentration in the coolant on time up to the maximum value of fuel burnup. The number of such calculations with different thermal-hydraulic parameters depends on demands for the global database generation.

The second step consists in collection and processing of the calculated data on fuel nuclide composition. Obtained nuclide compositions for all fuel rods as functions of exposure are averaged for several sets of selected rods having the similar history of exposure. The total amount of such sets does not exceed 5-7. As a rule, fuel rods of any set are selected according to their position in the fuel assembly (near the control rod guide, near the water gap between assemblies, etc.) The global database for the BARS fuel cycle modeling is generated by the TRIFON code for several fuel rods types differing by initial fuel enrichment, the exposure history, thermal-hydraulic parameters, etc. In practice of calculations it is enough to have no more than 50-60 types.

As a result, the global database contains several sets of Λ-matrices in the form of table functions of several parameters: fuel burnup, fuel temperature, moderator density, xenon concentration, and boron poisoning in the coolant and so on.

It should be noted that a nuclide composition prediction in burnable poison rods is a separate problem and is not considered in the present study.

5.2. Fuel Cycle Calculation with the Precalculated Database

This stage includes an LWR fuel cycle calculation by the BARS code using the global database precalculated by the TRIFON code. The core thermal-hydraulic calculations are carried out by the COTT code used as a coupled subroutine within the BARS code. Thermal-hydraulic parameters are calculated in the framework of assembly-by-assembly representation. (There is also a possibility to use pin-by-pin thermal hydraulics.) An iterative procedure for critical boron concentration in the coolant is used. At each burnup step, fuel burnup and xenon concentration are recalculated for each calculational node. The reactor power, inlet coolant temperature, initial boron concentration and control bank position are the input parameters in the BARS calculation.

6. FUEL CYCLE MODELING IN VVER. VALIDATION RESULTS

As it was mentioned, the pin-by-pin LWR fuel cycle model consists in two independent steps. For this reason a validation procedure was split into two stages; each of them may be considered as separate procedure and corresponding validation results may be of interest in other areas (for instance, a prediction of the nuclide composition in the high burnup fuel).

First stage dealt with the problem of prediction of nuclide composition in the fuel rods of a VVER under various operational conditions including geometrical and thermal-hydraulic effects on neutron spectrum in the fuel irradiated up to 60 MWd/kgU.

Second stage involved the modeling of the VVER-1000 fuel cycle itself by the BARS code using a neutron database prepared by the TRIFON code. The BARS input deck included available operational information on the fuel reloading scheme, soluble boron concentrations in the moderator during the fuel cycle, the reactor power history, axial positions of regulating banks of control rods, etc.

6.1. Validation of Calculational Model to Predict Fuel Nuclide Composition in VVER

Unfortunately, the experimental data on the VVER spent fuel nuclide composition available in literature are rather poor. As a rule, they include the data only for major actinides without any information on fission products playing an important role in the fuel cycle. Thus, these data do not allow validating a depletion code as a whole from the point of view of calculational accuracy in prediction of fission products composition. In this case it was worth to use calculational benchmarks aimed to compare capabilities of different depletion codes with various neutron data libraries. Another reason to use them was a possibility to analyze uncertainties due to different factors: neutronic and depletion models, libraries, etc.

As a result, it has been chosen the following validation database:

- VVER-440 burnup credit calculational benchmark CB2 (Ref. 24);
- a set of measured data for the nuclide composition of the high burnup spent fuel for VVER-440 and VVER-1000 reactors (Refs. 25 and 26).

6.1.1. CB2 Calculational Benchmark

This benchmark has been prepared in 1997 in the collaboration with the OECD/NEA/NSC Burnup Credit Criticality Benchmarks Working Group (Ref. 24). Reference 24 gives a detailed specification of this benchmark and contains 10 calculational sets obtained from 9 institutes of 7 countries. These data were calculated using modern depletion codes, such as CASMO-4, SCALE 4.3, WIMS7, HELIOS, etc. Depletion calculations for VVER-440 fuel pin cell were carried out for two burnup values: 30 and 40 MWd/kgU. Total number of nuclides which concentrations are given is 26 including 15 fission products.

In our study the calculational set obtained by the HELIOS (version 1.5) code was chosen as a reference one for validation because of the neutron library used by HELIOS was based on the same ENDF/B-VI file used also in the TRIFON code library. This fact allowed us to minimize the calculational uncertainty due to differences in the neutron libraries used by both codes.

The BARS-TRIFON results were calculated under the following conditions:

- number of energy groups in BARS: 5;
- number of energy groups in TRIFON: 260;
- numbers of burnup steps (recalculations of database) : 30 (for 30 MWd/kgU) and 40 (40 MWd/kgU).

The BARS-TRIFON code calculated the nuclide composition (except for ^{101}Ru that is not included in burnup chains) for each fuel rod within the fuel assembly and then the averaged data for selected nuclides were compared with the HELIOS results. The averaged results and the relative deviations (ε) are presented in Table 6.1.

Table 6.1 Comparison of the Calculational Results from HELIOS and BARS-TRIFON

Nuclide	Burnup = 30 MWd/kgU			Burnup = 40 MWd/kgU		
	HELIOS	BARS	ε (%)	HELIOS	BARS	ε (%)
^{235}U	2.894-4*	2.887-4	-0.2	1.931-4	1.929-4	-0.1
^{236}U	9.378-5	9.402-5	0.3	1.065-4	1.073-4	0.7
^{238}U	2.158-2	2.157-2	-0.01	2.139-2	2.138-2	-0.01
^{237}Np	8.540-6	7.714-6	-9.7	1.213-5	1.087-5	-10.4
^{238}Pu	2.541-6	2.363-6	-7.0	5.055-6	4.641-6	-8.2
^{239}Pu	1.362-4	1.386-4	1.8	1.420-4	1.456-4	2.5
^{240}Pu	4.475-5	4.822-5	7.7	5.734-5	6.243-5	8.9
^{241}Pu	2.829-5	2.775-5	-1.9	3.691-5	3.653-5	-1.0
^{242}Pu	7.231-6	7.194-6	-0.5	1.351-5	1.353-5	0.1
^{241}Am	8.653-7	8.307-7	-4.0	1.358-6	1.306-6	-3.8
^{243}Am	1.389-6	1.339-6	-3.6	3.362-6	3.255-6	-3.2
^{95}Mo	3.402-5	3.440-5	1.1	4.537-5	4.569-5	0.7
^{99}Tc	3.980-5	3.936-5	-1.1	5.134-5	4.998-5	-2.6
^{103}Rh	2.096-5	2.159-5	3.0	2.669-5	2.729-5	2.2
^{109}Ag	3.175-6	3.053-6	-3.9	4.745-6	4.508-6	-5.0
^{133}Cs	4.310-5	4.203-5	-2.5	5.533-5	5.308-5	-4.0
^{143}Nd	2.931-5	2.947-5	0.5	3.497-5	3.504-5	0.2
^{145}Nd	2.328-5	2.353-5	1.0	2.930-5	2.947-5	0.6
^{147}Sm	2.595-6	2.554-6	-1.6	3.603-6	3.470-6	-3.7
^{149}Sm	1.046-7	1.067-7	2.0	1.018-7	1.037-7	1.8
^{150}Sm	9.347-6	9.188-6	-1.7	1.256-5	1.223-5	-2.6
^{151}Sm	5.037-7	5.340-7	6.0	5.649-7	6.022-7	6.6
^{152}Sm	3.705-6	3.982-6	7.5	4.535-6	4.921-6	8.5
^{153}Eu	3.550-6	3.702-6	4.3	5.108-6	5.354-6	4.8
^{155}Gd	1.619-9	1.504-9	-7.1	2.579-9	2.491-9	-3.4

*Read as $2.894 \cdot 10^{-4}$

Based on the comparison of these data the following conclusions could be given:

- the deviations for major fissionable nuclides did not exceed 0.2% (for ^{235}U), 2.5% (for ^{239}Pu), 1.9% (for ^{241}Pu) and 0.01% (for ^{238}U);
- the maximum deviations for actinides were observed for ^{237}Np (10%), ^{240}Pu (9%) and ^{238}Pu (8%);
- the mean deviations for fission products did not exceed 4% (except for ^{151}Sm, ^{152}Sm and ^{155}Gd) and the maximum deviation was 8.5% for ^{152}Sm.

It should be noted that the comparison with some other results from Reference 24 indicated more significant deviations (especially, for ^{155}Gd), that may be explained to some extend by using different calculational approaches or neutron libraries.

6.1.2. Experimental Data for Spent Fuel of VVER-440 and VVER-1000

The experimental data for the VVER spent fuel nuclide composition consisted in 5 sets for fuel samples from the Novovoronezh NPP Unit 5 VVER-1000 and 1 set for a fuel sample from the Kola NPP Unit 3 VVER-440. Initial enrichment of the fuel samples was 3.6 or 4.4 wt.%. The fuel burnups were in the range of 44 to 60 MWd/kgU. The reason why the data for such high burnup fuel were chosen in this validation was to specify the code capabilities in prediction of long-duration fuel cycles in VVERs.

The tested samples of the VVER-1000 belonged to 4 fuel rods of the same fuel assembly irradiated during 3 fuel cycles. Non-symmetrical arrangement of the fuel rods and control rod guide tubes in the fuel assembly for Novovoronezh NPP Unit 5 VVER-1000 differs from that for a standard VVER-1000. It can be seen in Figure 6.1 where the considered fuel rods are indicated using accepted for VVER notation. The assembly contained fuel rods with initial enrichment of 4.4 wt.% except for peripheral row with enrichment of 3.6 wt.%.

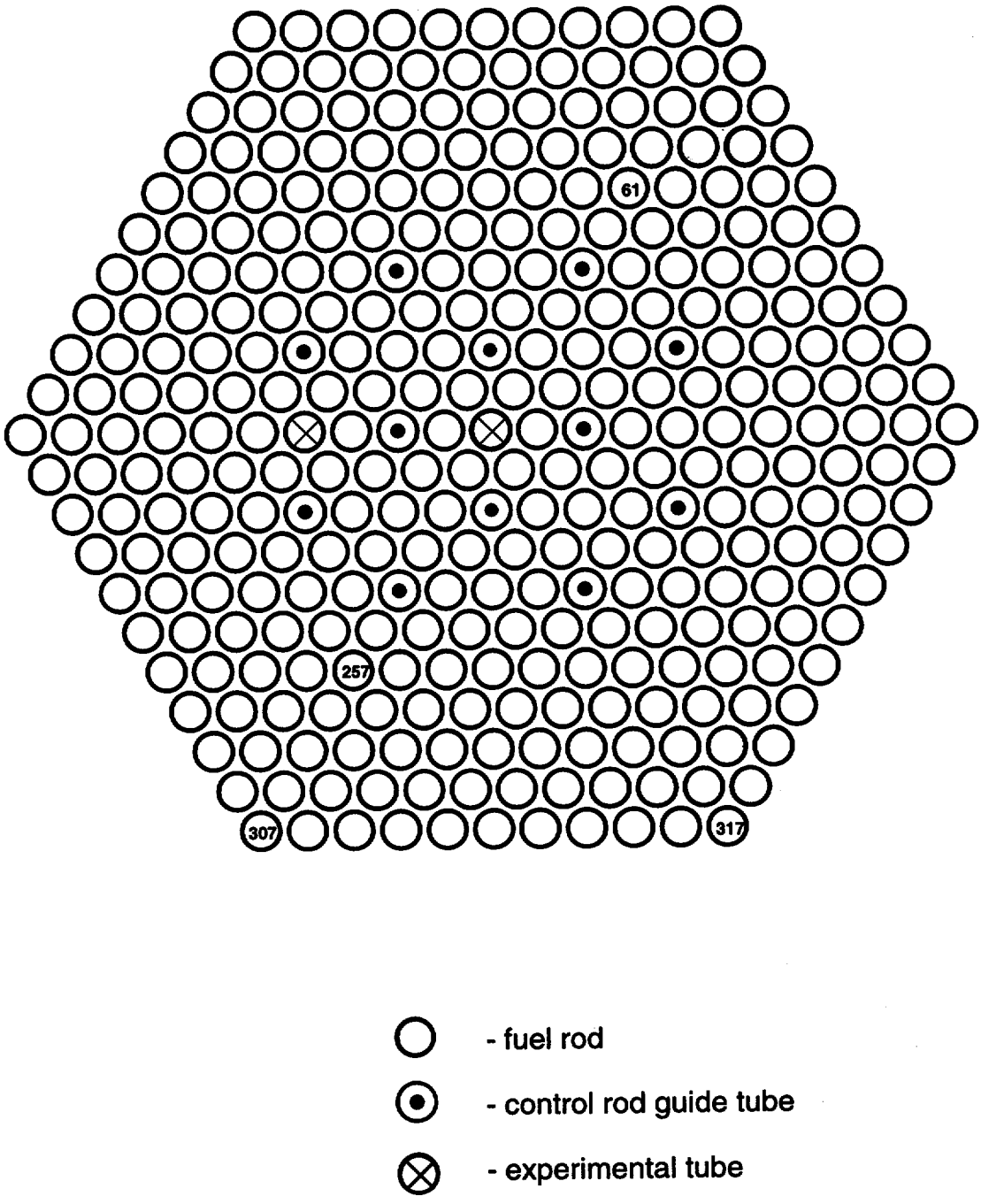

Figure 6.1 Layout of the Fuel Assembly of the Novovoronezh NPP Unit 5

The VVER-440 fuel assembly of the Kola NPP Unit 3 was irradiated during 5 fuel cycles. It consisted in 126 fuel rods and the central Zr-tube. The tested sample belonged to the fuel rod No.81 that was located at the outer row near the corner fuel rod.

All of the samples were cut approximately from the central part of the fuel rod. References 25 and 26 contain the nuclide compositions of considered samples in terms of kilograms per tone of initial U (for high burnup fuel 1 MWd/kgU is equal to approximately 0.97 kg/tU.)

Due to the evident non-physical discrepancy and poor accuracy, the data for ^{241}Am, ^{242}Cm and ^{244}Cm were not considered in the comparison.

The BARS-TRIFON results were calculated under the following conditions:

- number of energy groups in BARS: 5;
- number of energy groups in TRIFON: 280;
- number of burnup steps: 60 (for 60 MWd/kgU).

Operational data on the primary coolant thermal hydraulics, the boric acid concentrations in the coolant and duration of the fuel cycles including downtime between cycles were taken into account. Cooling times before measurements were 3.4 years for the VVER-1000 fuel rods and 7.1 years for the VVER-440 fuel rod.

Calculational results and the relative deviations (ε) are presented in Tables 6.2 through 6.4. Notation of the experimental samples was given accordingly to corresponding fuel rod numbers; two samples from the same fuel rod No.307 were indicated as 307a and 307b (the last sample was cut 70 cm below the middle point on the fuel rod active length). Experimental uncertainty is given in the brackets after the value as an error in the last digit.

Table 6.2 Comparison of the Calculational and Measured Data (kg/tU) for the Fuel Samples with Initial Enrichment of 4.4 wt% (Novovoronezh NPP Unit 5 VVER-1000)

Nuclide	Sample No.61			Sample No.257		
	Measured	BARS	ε (%)	Measured	BARS	ε (%)
^{235}U	11.7 (1)*	10.8	-8.2	8.80 (7)	8.58	-2.5
^{236}U	5.33 (6)	5.67	6.4	6.23 (6)	5.94	-4.6
^{238}U	927 (1)	927	0.0	924 (1)	923	-0.1
^{238}Pu	0.27 (2)	0.20	-26.	0.32 (2)	0.26	-18.
^{239}Pu	5.64 (6)	5.80	2.8	5.38 (7)	5.78	7.4
^{240}Pu	2.29 (3)	2.41	5.2	2.55 (3)	2.65	3.9
^{241}Pu	1.51 (2)	1.42	-6.0	1.60 (1)	1.52	-5.0
^{242}Pu	0.56 (1)	0.60	7.1	0.79 (1)	0.77	-2.5
^{243}Am	0.15 (1)	0.14	-8.2	0.21 (1)	0.19	-7.2
Burnup	45. (2)	45.0	-	50. (2)	50.5	-

*Read as 11.7 ± 0.1

Table 6.3 Comparison of the Calculational and Measured Data (kg/tU) for the Fuel Samples with Initial Enrichment of 3.6 wt% (Novovoronezh NPP Unit 5 VVER-1000)

Nuclide	Sample No.307a			Sample No.307b			Sample No.317		
	Measured	BARS	ε (%)	Measured	BARS	ε (%)	Measured	BARS	ε (%)
^{235}U	4.35 (3)*	4.16	-4.3	3.69 (2)	3.96	7.3	3.60 (4)	3.77	-4.7
^{236}U	4.92 (3)	4.98	1.2	5.38 (4)	4.99	-7.2	4.82 (3)	5.00	3.7
^{238}U	927 (1)	926	-0.1	927 (1)	926.	-0.1	928 (1)	925	-0.3
^{238}Pu	0.31 (2)	0.29	-6.2	0.32 (2)	0.30	-6.2	0.31 (2)	0.31	0.1
^{239}Pu	5.00 (5)	5.14	2.8	5.10 (5)	5.12	0.4	5.18 (4)	5.11	-1.4
^{240}Pu	2.62 (3)	2.85	8.8	2.73 (2)	2.88	5.5	2.67 (3)	2.90	8.6
^{241}Pu	1.64 (2)	1.50	-8.5	1.67 (1)	1.50	-10.	1.72 (2)	1.52	-11.
^{242}Pu	1.12 (1)	1.05	-6.2	1.12 (1)	1.08	-3.6	1.19 (1)	1.12	-5.9
^{243}Am	0.29 (2)	0.28	-1.2	0.29 (1)	0.30	1.7	0.31 (1)	0.31	0.1
Burnup	52. (2)	52.4	-	53. (2)	53.1	-	54. (1)	54.0	-

*Read as 4.35 ± 0.03

Table 6.4 Comparison of the Calculational and Measured Data (kg/tU) for the Fuel Sample with Initial Enrichment of 4.4 wt% (Kola NPP Unit 3 VVER-440)

Nuclide	Sample No.81		
	Measured	BARS	ε (%)
^{234}U	0.22 (2)*	0.17	-20.
^{235}U	4.71 (4)	5.03	6.9
^{236}U	6.65 (5)	6.48	-2.6
^{238}U	915.4 (1)	914.7	-0.1
^{238}Pu	0.57 (1)	0.43	-26.
^{239}Pu	5.75 (5)	5.89	2.4
^{240}Pu	3.03 (3)	3.31	9.2
^{241}Pu	1.32 (2)	1.30	-2.3
^{242}Pu	1.27 (2)	1.12	-11.
Burnup	61. (1)	61.0	-

*Read as 0.22 ± 0.02

Based on the data for high burnup fuel presented in Tables 6.2 through 6.4, the following conclusions could be given:

- the mean deviations for major fissionable nuclides did not exceed 6% (for ^{235}U), 3% (for ^{239}Pu), 7% (for ^{241}Pu) and 0.1% (for ^{238}U);
- the maximum deviations for actinides were observed for ^{238}Pu (26%), ^{241}Pu, ^{242}Pu (11%) and ^{240}Pu (9%);
- all the deviations are greater compared with the calculational benchmark for the VVER-440 fuel irradiated to 30 and 40 MWd/kgU.

Thus, it is safe to conclude that the BARS-TRIFON code models the nuclide composition of the VVER fuel with reasonable accuracy when compared with the measured data up to the fuel burnup of 60 MWd/kgU. The burnup chains model implemented in the code provides very good accuracy in prediction of the fission products in the VVER spent fuel.

6.2. Validation of Calculational Model for VVER-1000 Fuel Cycle

Below the BARS calculational results for modeling of first 3 fuel cycles in the Kozloduy NPP Unit 5 are presented. This unit has a VVER-1000 reactor operated in 2-year cycle regime since 1988. Initial loading of the core consisted in the fuel of 3 different enrichments: 2% (79 assemblies), 3% (42 assemblies) and 3.3% (36 assemblies, among them 6 assemblies with 3%-fuel at the periphery). After the first 2 cycles 2%- and 3%-fuel assemblies were charged and replaced by the 3.3%-fuel assemblies (except for a few assemblies with 3%-fuel at the periphery).

Reference 27 contains a brief description of operational parameters for first 3 cycles: effective lengths of the cycles, fuel reload maps, the tables of thermal-hydraulic (the coolant inlet temperature and flow) and operational (core power, boron poisoning and positions of the regulating banks in the core) data. Thermal-hydraulic parameters were more or less stable during the cycles. The coolant flow was approximately (66.5 ± 0.5) kilotons per hour. The mean values for the coolant inlet temperature (with deviation of 2°C during the cycles) were:

- 286°C in the first cycle (at the last 6 days of this cycle the temperature was reduced by 4-5°C);
- 282°C in the second cycle;
- 284°C in the third cycle.

Unfortunately, all the tables were given as a function of effective power days (not calendar days). For this reason it was impossible to model the cycles using detailed data on core power and regulating banks positions. Another reason was a very complicated behavior of core power (Figure 6.2) with frequent changes in regulating banks position (several regulating banks were used).

In this study it was assumed that the reactor was operated during all the cycles at rated power of 3000 MW with partly inserted 6 control rods of regulating bank No.10 located at the central part of the core. According to the rated power, axial location for these control rods was chosen as 260-270 cm from the bottom of the core.

The coolant inlet temperature and flow were constant during each cycle (the reduction in inlet temperature at the end of the first cycle was effectively taken into account as additional full power days due to negative temperature feedback). The burnup calculational step was 20 days in all calculations. The boric acid concentration in the coolant was a key parameter in this validation and the length of the fuel cycle was determined as a time period from the beginning of the cycle up to a time moment when the boric acid concentration reached the zero level.

BARS calculational parameters were as follow:

- number of energy groups: 5;
- number of axial fuel zones with different properties: 15;
- number of axial harmonics: 16.

Figure 6.3 through 6.5 illustrate the boron concentration behavior during the cycles. The measured data are given as circles and the calculational results – as bold curves. As it can be seen from Figure 6.4, the most spread of the measured data was observed for the first quarter of the second cycle. The calculational dependence was practically linear during the cycles.

Table 6.5 gives the comparison between the operational and calculational cycle lengths in terms of full power days (FPD).

Table 6.5 Lengths (FPD) of First 3 Cycles in the Kozloduy NPP Unit 5

Cycle No.	Operation	Calculation	Deviation
1	296.7	294.3	-2.4
2	324.5	317.7	-6.8
3	317.8	320.3	2.5

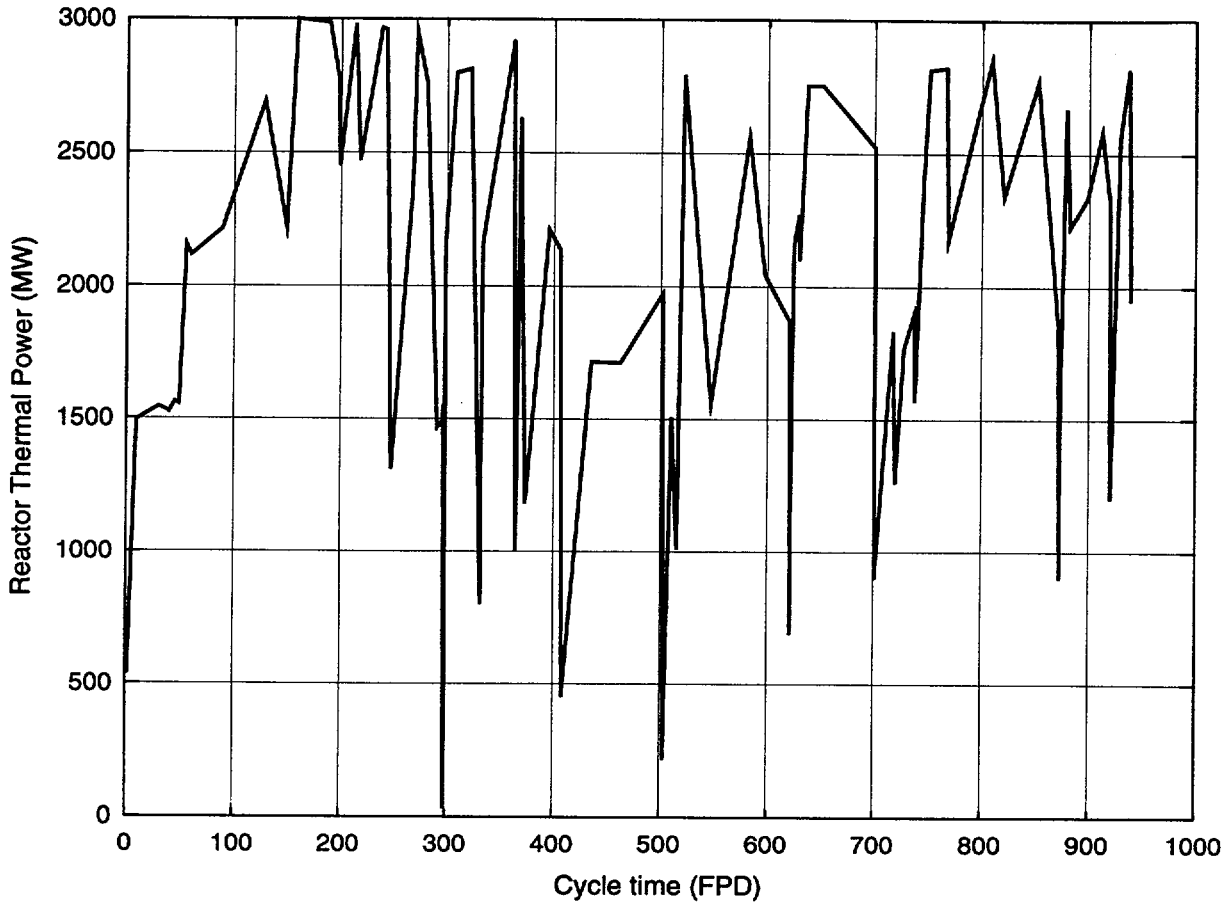

Figure 6.2 Reactor Power During First 3 Cycles

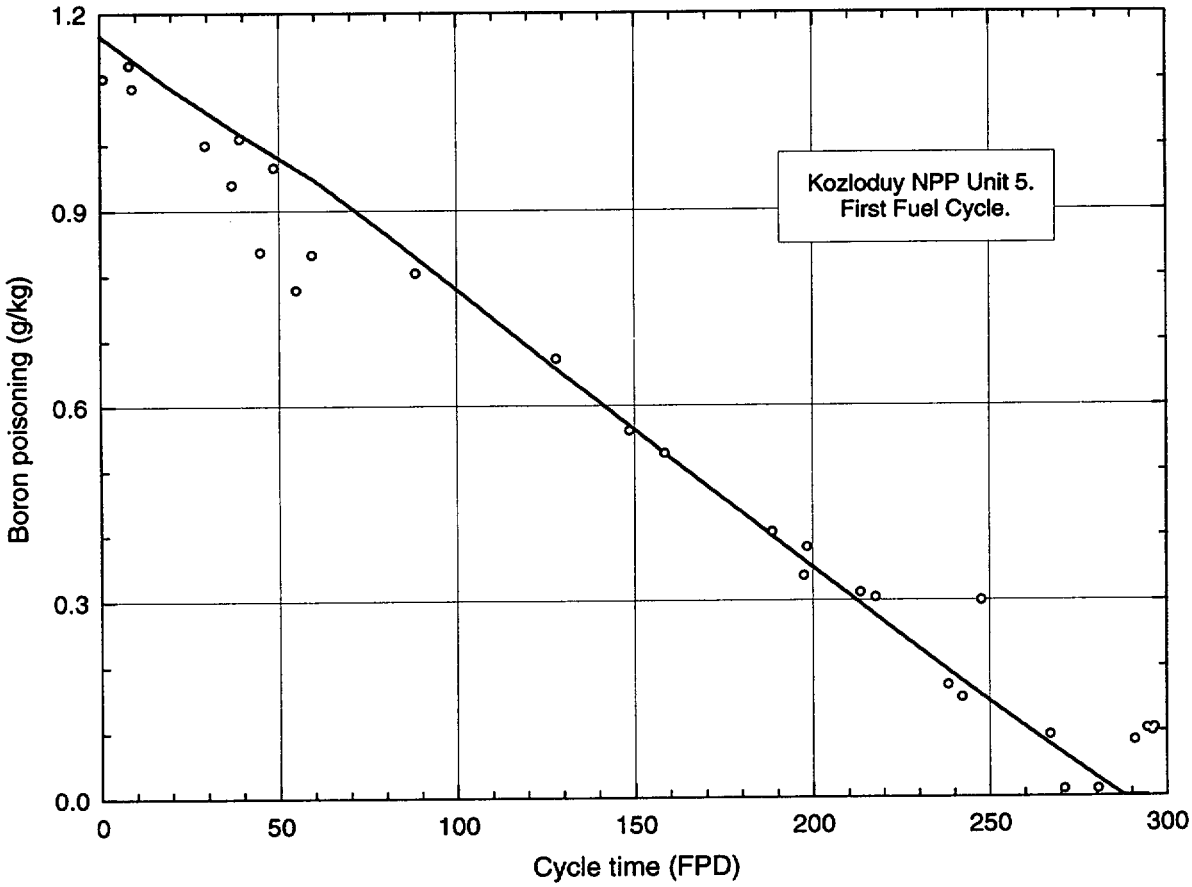

Figure 6.3 Boron Concentration in the Coolant During the First Cycle

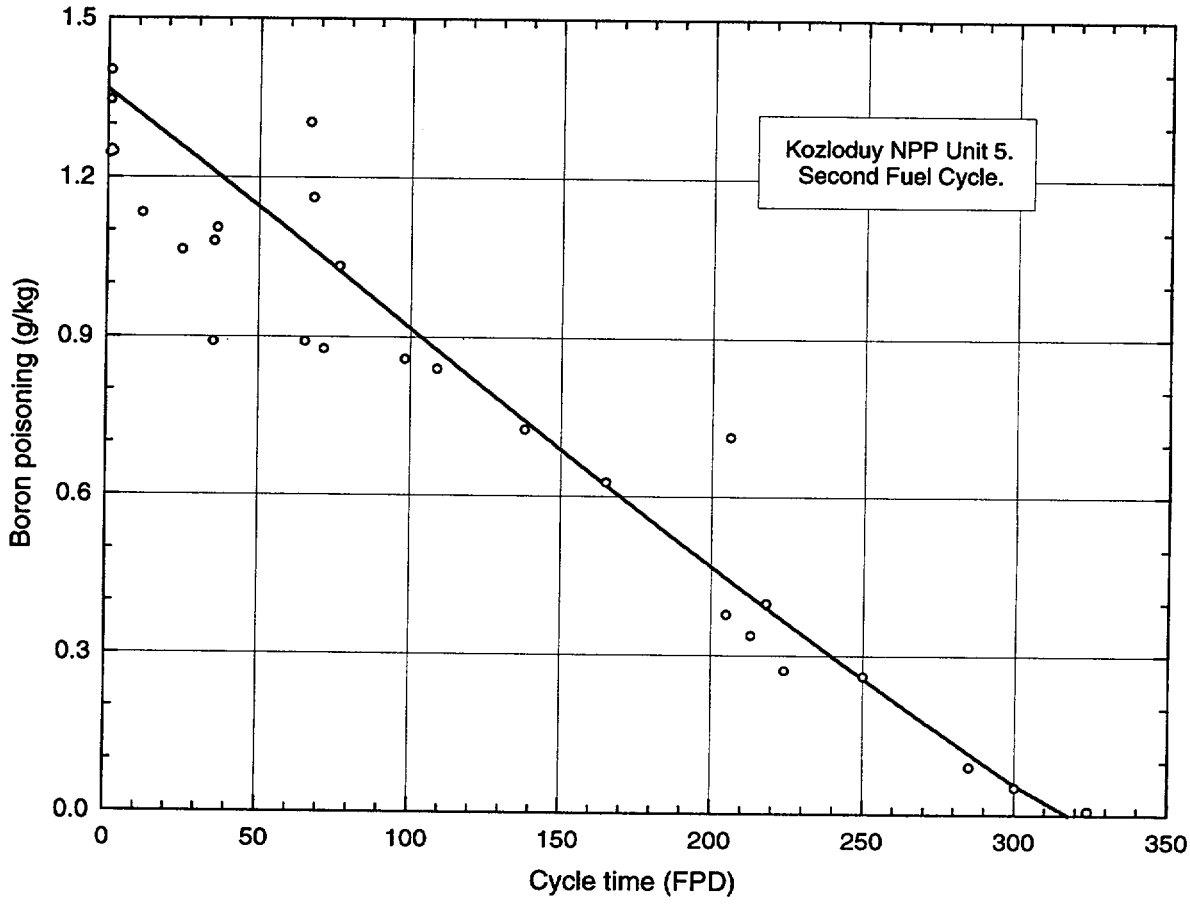

Figure 6.4 Boron Concentration in the Coolant During the Second Cycle

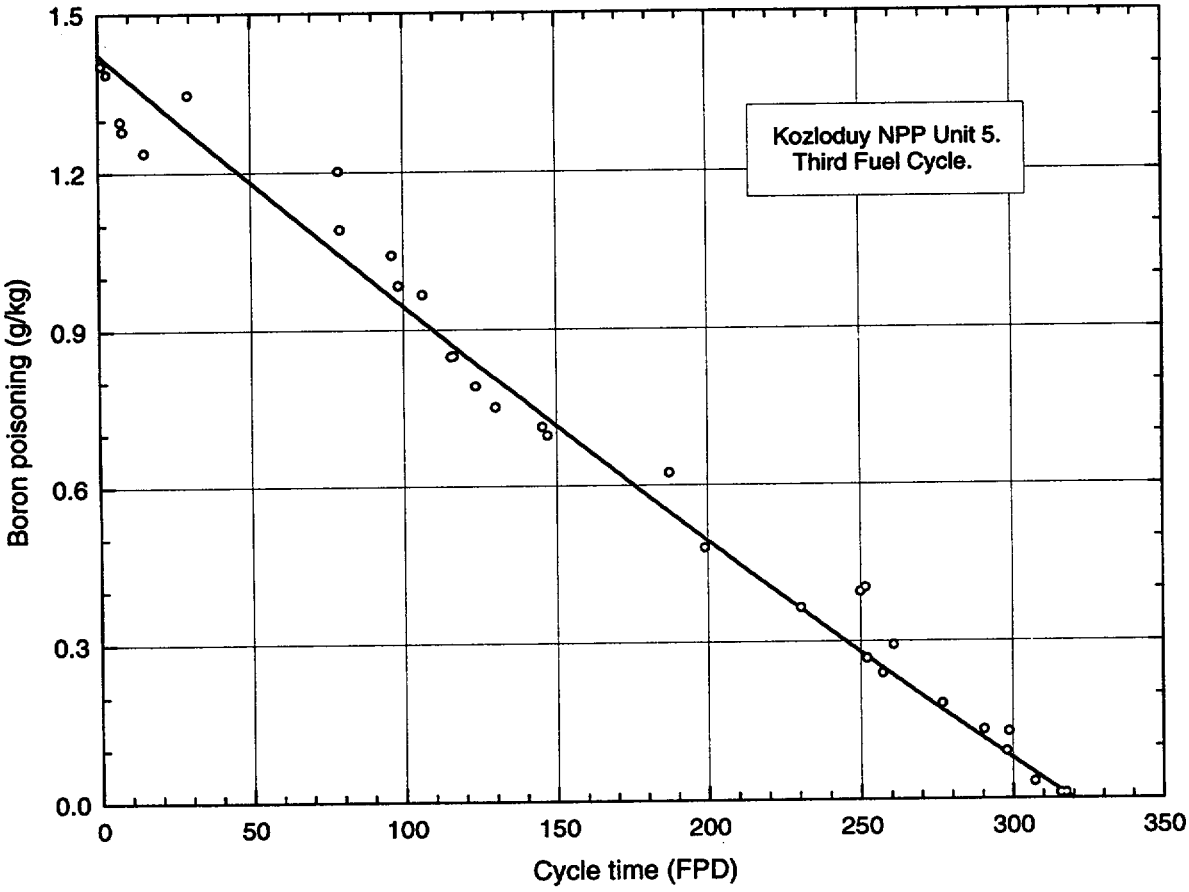

Figure 6.5 Boron Concentration in the Coolant During the Third Cycle.

For the first cycle the calculational value was effectively increased by 6.5 FPD due to the moderator temperature effect. This increment $\Delta\tau$ was estimated accordingly to the following simple formula:

$$\Delta\tau = \Delta T \, \alpha_t / \alpha_B / c_B',$$

where

ΔT is the moderator temperature decrement,

α_t is the moderator temperature coefficient of reactivity,

α_B is the boron coefficient of reactivity,

c_B' is the derivative of the boron concentration as a function of FPD.

Substitution of ΔT = 4.5 K and the corresponding EOC parameters (α_t = -61 pcm/K; α_B = -0.11 1/(g/kg); c_B'= 0.0038 (g/kg)/FPD) gave $\Delta\tau$ = 6.5 FPD.

From the presented comparison of the calculational and operational data on the cycle lengths, the following conclusions may be derived:

- a good agreement was obtained for the cycle lengths; the mean deviation over 3 cycles did not exceed 4 FPD;
- the boron concentration behavior during the cycles agreed with the operational data, though it was difficult to give quantitative estimate of this agreement because of the very complicated history of the reactor power;

Nevertheless, it is clear that the comprehensive validation has to include the detailed modeling of the fuel cycle with corresponding changes in such parameters as inlet coolant temperature, reactor power, control banks position, etc. Such calculations, of course, are very expensive because they demand a lot of calculational steps.

7. CALCULATION OF A VVER-1000 REA. EFFECT OF PIN-BY-PIN FUEL POWER AND BURNUP REPRESENTATION

In recent calculational studies of power excursions in VVER-1000 core containing only fresh fuel, a number of interesting results was found (Ref. 28). Among them the following ones may be pointed out:

- ejection of a peripheral control rod resulted in a very complicated pin-by-pin power distribution in assemblies directly adjacent to the accident one;
- the hottest fuel rod did not necessarily belong to assembly with peak power;
- fuel assemblies, adjacent to the accident one from the one side and to the reflector from the other, with relatively low power contained fuel rods with power exceeded maximum value for fuel rods in assembly with peak power.

This Section describes an analogous study of a VVER-1000 but with burnup core. Two comparative calculations were carried out by the RELAP5-BARS coupling code for the South Ukrainian NPP Unit 1 VVER-1000 at the end of the third fuel cycle. The main difference between these calculations was in fuel burnup representation. Two types of the core were considered: one with pin-by-pin burnup distribution and another - with assembly averaged burnup when all nodes of any axial layer within any fuel assembly were of the same burnup. Main goal of this comparison was to understand how the burnup representation could influence the consequences of the VVER REA from the point of view of the peak fuel enthalpy.

The South Ukrainian NPP Unit 1 was operated in 2-year cycle regime without any burnable poison rods in the core. Calculational procedure and main results for the first 3 cycles were identical to those described in previous Section. Calculational average burnup of the core at the end of the cycle was 21 MWd/kgU with peak burnup of 37.5 MWd/kgU for the calculational node in the central part of the core.

Neutronic calculations by the BARS code were carried out using 4 energy groups, 6 groups of delayed neutron precursors and 16 axial harmonics. The thermal-hydraulic model of the core used by the RELAP5 code was identical to that described in Reference 28 with selected the hottest fuel pin as separate heat structure.

7.1. Initial Conditions of the Accident

The initial thermal-hydraulic conditions in the reactor corresponded to hot zero power (HZP) startup. The reactor power was 10^{-6} of the rated power, and the coolant inlet temperature and flow rate were 287°C and 17 t/s respectively.

A key factor in REA analysis is the worth of ejected control rod. At normal operational conditions the worth of any rod does not exceed 1$. Because the goal of this study was to analyze consequences of a REA at conservative initial reactor conditions with the ejected control rod worth of 1.2$, the initial control rod pattern was changed. There are 61 control rods grouped in 10 different banks in the VVER-1000 core. In this study it was assumed that 18 control rods of 3 banks in the central part of the core and 18 control rods (including the accident rod) of 3 peripheral banks were fully inserted. Figure 7.1 presents location of inserted control rods before the accident. As shown in the figure, the control rod pattern was non-symmetrical because one control rod located near the ejected one was assumed as stuck out. This asymmetry resulted in required worth of the ejected control rod. It should be mentioned that such an approach is more realistic compared with artificial adjustment of neutron cross sections for this region to reach the desired value of the control rod worth.

7.2. Analysis of Rod Ejection Accident Modeling

As it was above mentioned, two identical calculations were done. Case 1 – with the pin-by-pin burnup distribution and Case 2 – with the assembly averaged one. Thus, the RELAP-BARS input decks for both variants differed only by the initial burnup distributions.

First of all, two calculations of HZP steady state were performed. Comparison of the results gave the following maximum deviations in the neutronic parameters:

- assembly-by-assembly power distribution: 4%;
- control rods banks worth: 4%;
- worth of a single control rod: 7%;
- delayed neutron fraction: 0.2%;
- prompt neutron life time: 0.2%.

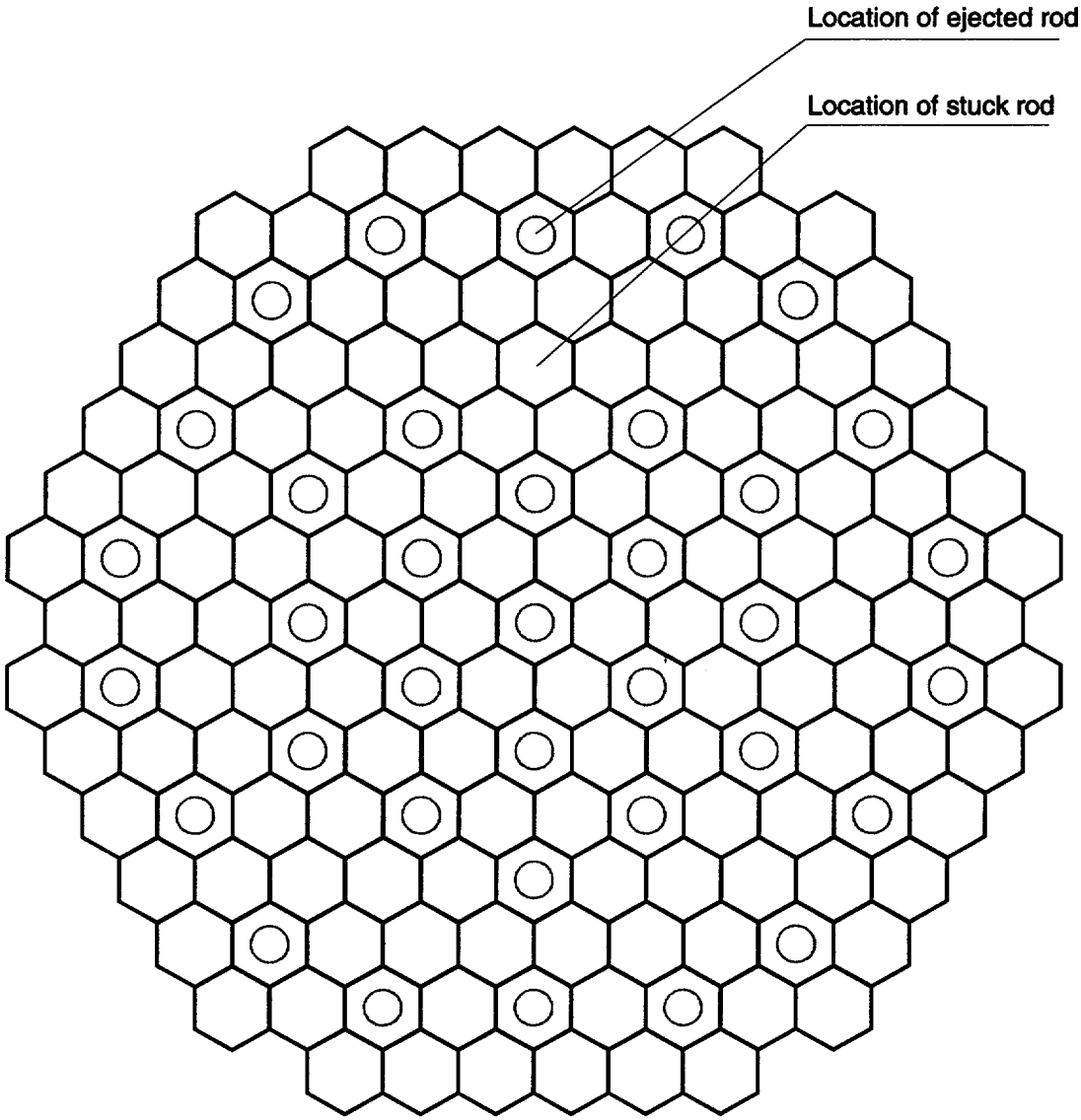

Figure 7.1 Control Rod Pattern in the VVER-1000 Core Before REA

The deviation in the worth of the ejected rod was found as no more than 0.2%. Thus, uncertainties in REA calculational results due to that deviation were expected as minimal.

The accident was initiated at time zero with the peripheral control rod ejection at a speed of 35.4 m/s (thus, the control rod was ejected during 0.1 s). The maximum value of reactivity of approximately 1.21$ was reached practically just after the full withdrawal of the control rods at about 0.2 s. The reactor power reached a peak value at 0.4 s, after that, due to the large negative Doppler feedback, the power excursion was terminated. During the transient no scram was assumed. Total duration of the calculated transient was chosen as 3 s.

Calculational results for both cases were found as very close each other. Table 7.1 presents a comparison of some neutronic and thermal-hydraulic parameters for both cases during the transient.

Table 7.1 Comparison of the REA Calculational Results for Pin-by-Pin (Case 1) and Average (Case 2) Burnup Models

Parameter of transient	Case 1	Case 2	Deviation
Maximum reactivity ($)	1.2102	1.2076	- 0.2 %
Peak power (% of rated power)	113.5	112.2	- 1.1 %
Time of power peak (ms)	402	403	1 ms
Pulse width (ms)	85.3	85.9	0.7 %
Prompt neutron life time for peak power (ms)	0.0281	0.0280	- 0.4 %
Delayed neutron fraction for peak power (%)	0.5810	0.5822	0.2 %
Power at t=3 s (% of rated power)	6.02	6.05	0.5 %
Enthalpy increment for the hottest pin (cal/g)	22.1	21.9	- 1.1 %
Fuel temperature for the hottest pin (K)	861	858	- 3 K

Figure 7.2 shows the reactor power and the reactivity as functions of the time of the transient. Deviations of these parameters decreased by the end of transient (Table 7.1).

Fuel enthalpy increment (pellet radial average for any axial layer) which is a key factor in RIA analysis is shown in Figure 7.3. This figure shows also a relative deviation in the fuel enthalpy increment between both cases.

The pin-by-pin power distribution (one-half part of the core) is presented in Figure 7.4. As the figure shows this distribution is very complicated, especially near the ejected rod. In this region, each assembly adjacent to the reflector has a very large distortion in the power across the assembly. Average power of such assemblies was relatively small, but they contained the pins with more high power compared to those in the assembly with peak power (the accident assembly). This effect is a matter of principle in the comparison of two approaches: assembly-by-assembly and pin-by-pin.

From the data presented in Table 7.1 and Figures 7.2 and 7.3, the following major conclusion may be given: the deviations in the neutronic and thermal-hydraulic parameters due to different burnup representation model are rather small. As the possible reasons of such result, the following may be considered. In this study, the VVER-1000 core with very low average burnup (21 MWd/kgU) was analyzed. Besides, a VVER-1000 reactor operated in 2-year cycle regime does not contain burnable poison rods in the core.

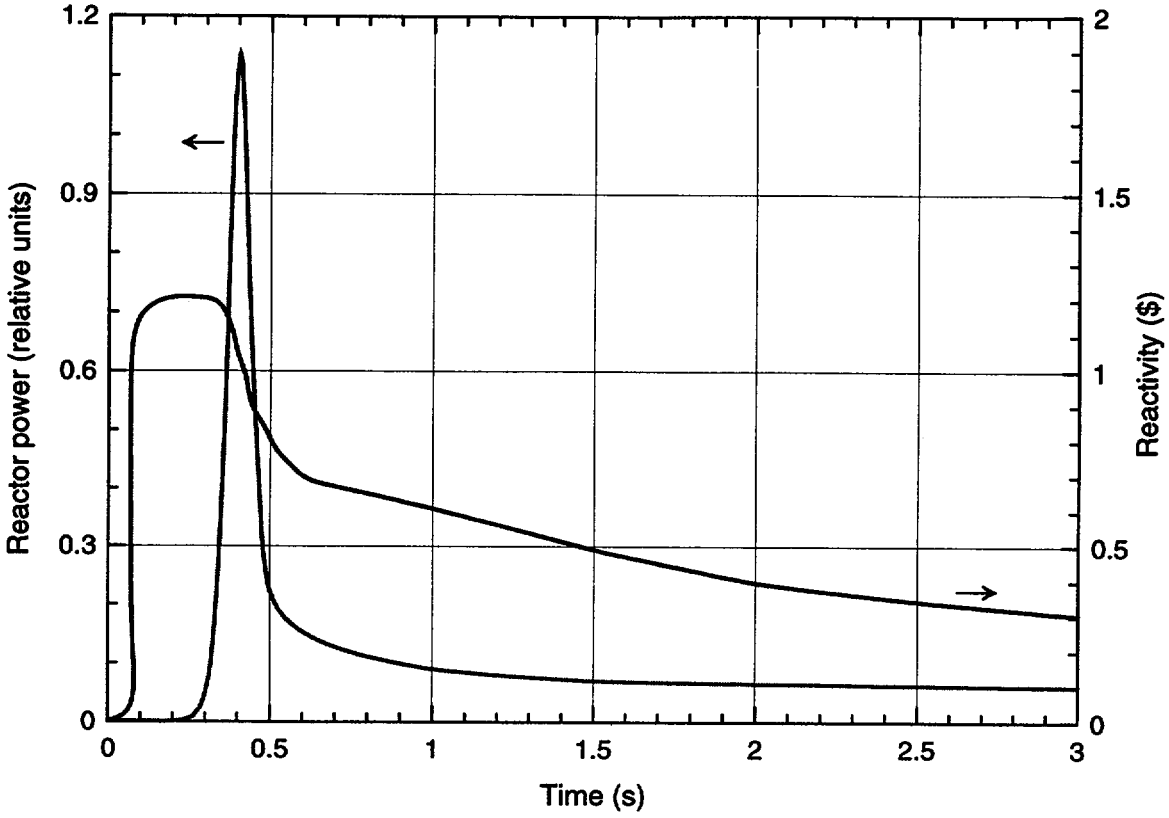

Figure 7.2 Reactor Power and Reactivity During REA

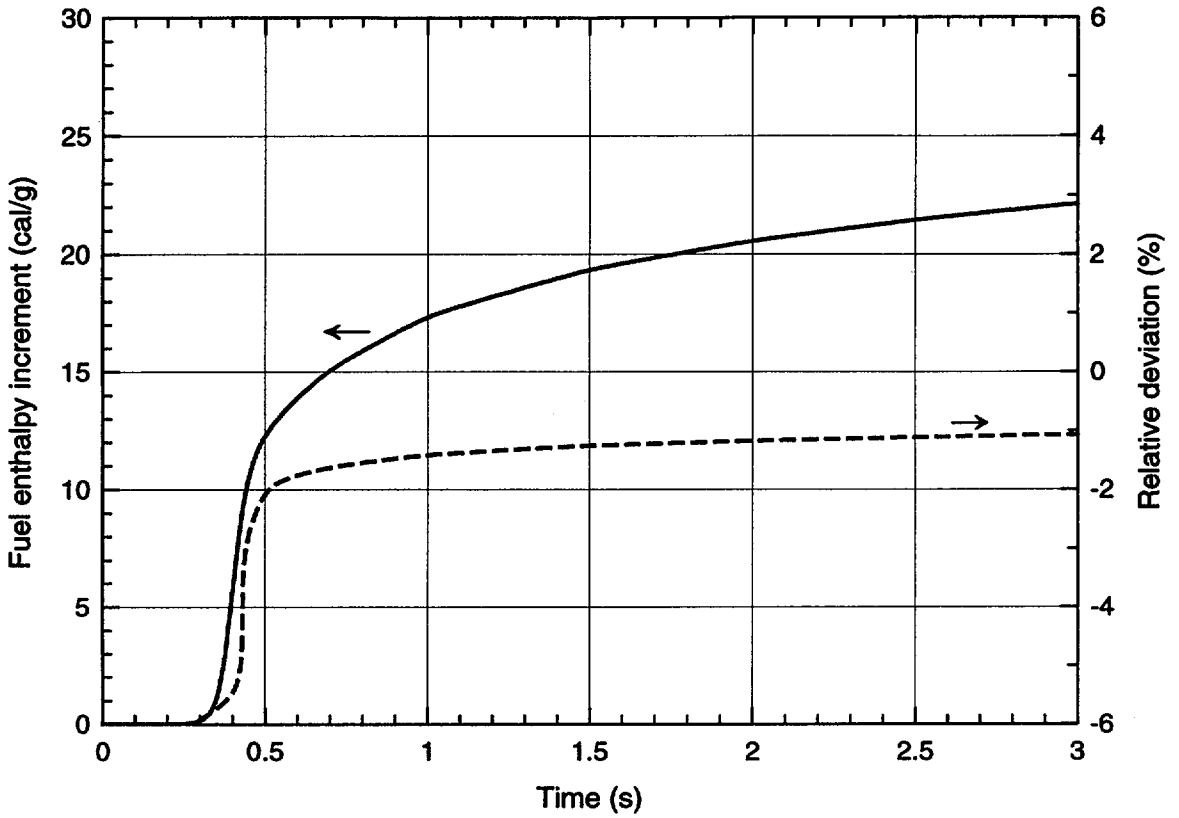

Figure 7.3 Fuel Enthalpy Increment and Its Relative Deviation During REA

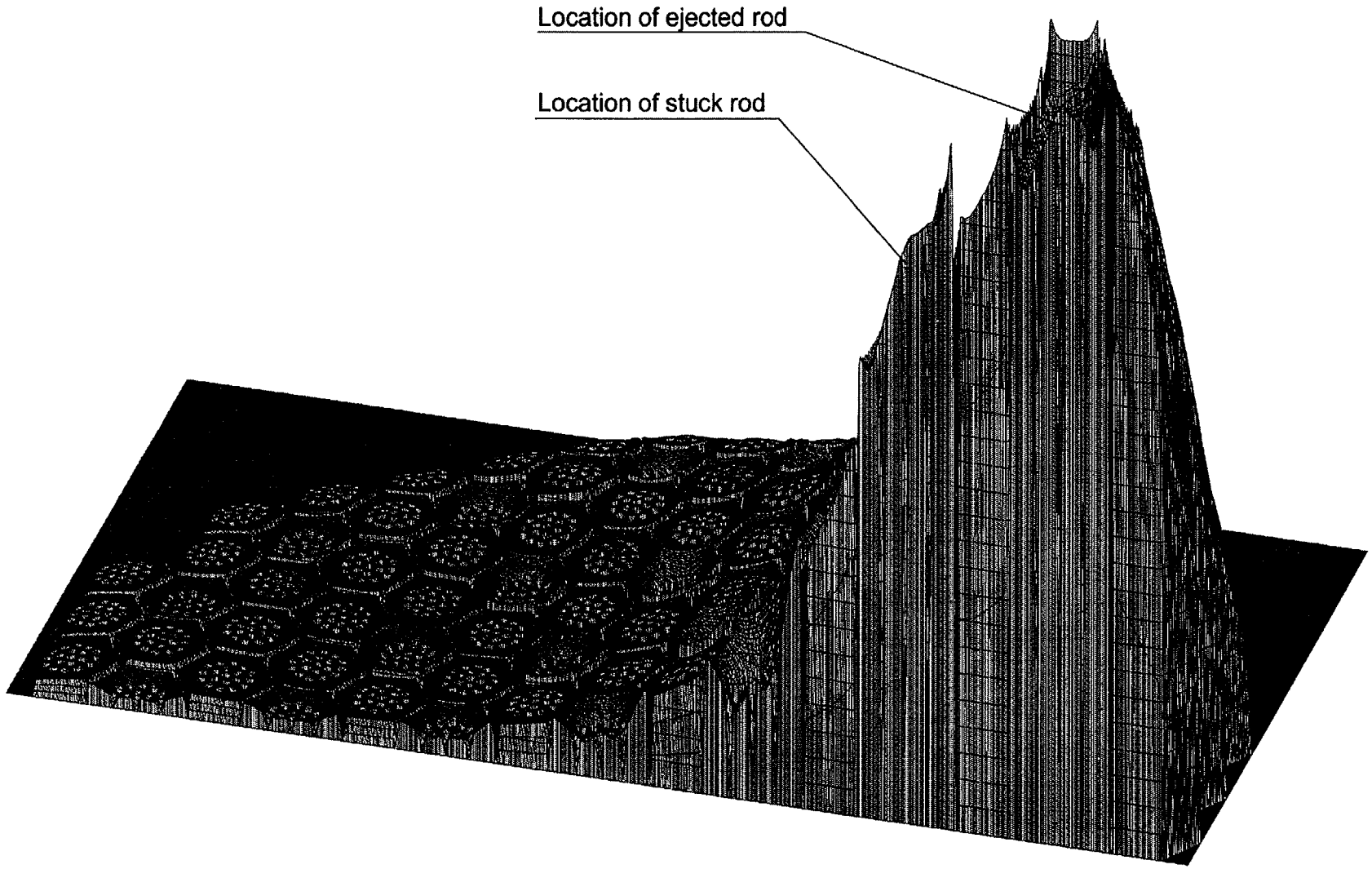

Figure 7.4 Pin-by-Pin Power Distribution After Rod Ejection

8. CALCULATION OF TMI-1 REA

This Section describes recent RELAP-BARS calculational efforts aimed to understand the uncertainty in analysis of the effect of the detailed intra-assembly fuel power and temperature representation on neutronic and thermal-hydraulic parameters during a PWR REA. The effect of the pin-by-pin power representation was studied by comparison of the RELAP-BARS results with the PARCS and CRONOS2 calculations. Analysis of the effect of intra-assembly fuel temperature representation was made using two different approaches in the calculation of the fuel temperature: assembly-by-assembly (Case 1) and pin-by-pin (Case 2). The last model is based on the fuel temperature reconstruction method described in Section 4. Both models used the same pin-by-pin power calculational approach. The major difference between two models was the representation of the fuel temperature within any assembly. In Case 1 the single axial distribution of the fuel temperature of the pin with averaged power was used for all pins within the assembly. While in Case 2 each fuel pin has its own axial fuel temperature distribution calculated using the corresponding power distribution.

The reactor model used in the RELAP-BARS calculations was based on the PWR of Three Mile Island Unit 1 that was chosen as an international benchmark (Ref. 29). The reactor core having one-eight symmetry contains fuel assemblies with fuel burnup ranged from 23 up to 58 GWd/t (at the end of the cycle). To generate neutron database for BARS, fuel nuclide compositions averaged over each assembly in each axial layer were used. This information was received from U.S. partners. Thus, fuel pins within each assembly in each axial layers had the same set of Λ-matrices.

Initial conditions were hot zero power (HZP) with 20 control rods of 3 regulating banks fully inserted in the core as shown on Figure 8.1. This figure indicates that all inserted control rods are located at assemblies with high burnup fuel. It is obvious that after withdrawal of one of them, peak power will be observed in any neighboring assembly having relatively low burnup. For instance, after withdrawal of peripheral rod N12 of Bank 7, peak power will be in assembly N13 with fuel burnup of 24 GWd/t.

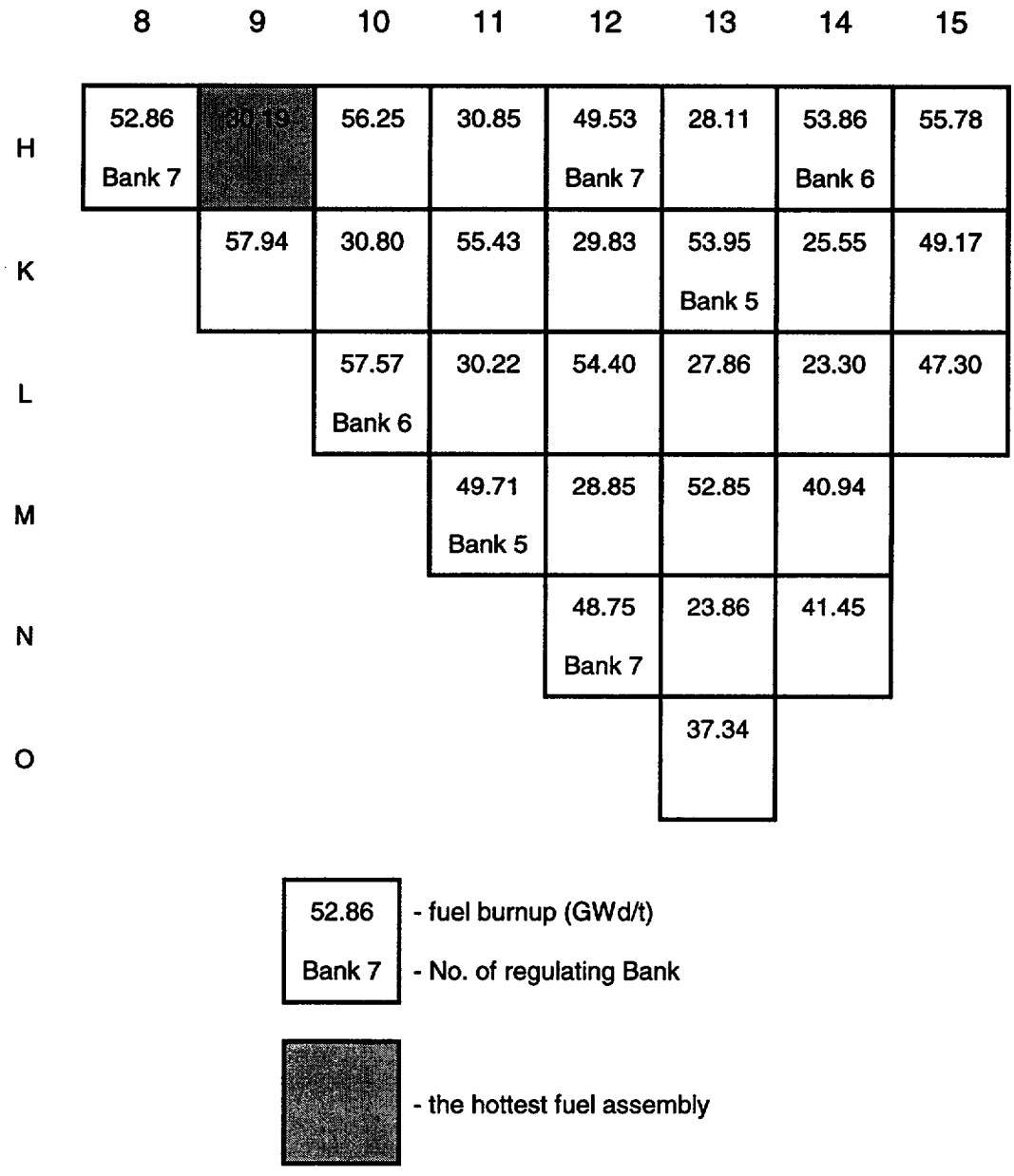

Figure 8.1 One-Eight Core Layout

In basis case, considered as a REA, after ejection of central rod H8, power (both assembly averaged and pin-by-pin) reaches its peak value in assembly H9. This unrodded assembly with average burnup of 30 GWd/t contains two hottest pins located near the water gap between both assemblies as shown on Figure 8.2.

8.1. Steady-State Calculations

Before REA modeling, a number of steady-state calculations were carried out using RELAP-BARS coupled code. Below a comparison of the different neutronic approaches concerning REA modeling is presented. There were two models: the pin-by-pin one (BARS) and assembly-by-assembly one (PARCS and CRONOS2).

The goal of such an intercomparison was to specify major differences in some neutronic and thermal-hydraulic parameters (power distribution, worth of the ejected control rod, the Doppler and moderator temperature coefficients of reactivity) which could effect on consequences of the REA.

It should be noted that PARCS and CRONOS2 used the same two-group cross sections generated with the CASMO-3 code (Ref. 10). As a result, steady state calculational data were very close for both codes. For this reason only the PARCS results were used in this intercomparison.

BARS calculational parameters were as follow:

- number of energy groups: 4;
- number of axial fuel zones with different properties: 24;
- number of axial harmonics: 20.

Table 8.1 summarizes basic steady state parameters calculated by BARS and PARCS with corresponding deviation of the BARS value from the PARCS one. Together with worth of regulating banks and single rods of Bank 7, this table contains data on axial peaking factors and reactivity coefficients: the Doppler one and the isothermal temperature coefficient (ITC).

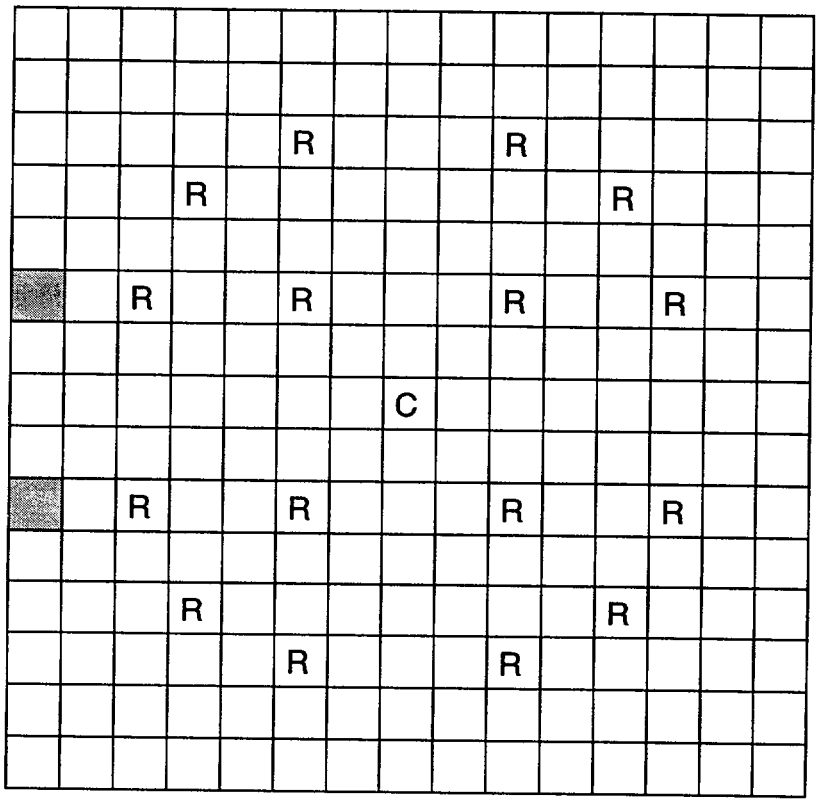

Figure 8.2 Layout of Assembly H9

Table 8.1 Steady-State Parameters

Parameter	PARCS	BARS	Deviation (%)
Worth of Bank 5 (pcm)	1423	1548	8.8
Worth of Bank 6 (pcm)	849	859	1.2
Worth of Bank 7 (pcm)	1050	1105	5.2
Worth of rod H8 (pcm)	347	338	-2.6
Worth of rod H12 (pcm)	188	202	7.4
Worth of rod N12 (pcm)	344	543	58
Axial peaking factor	2.65	3.10	17
Doppler coefficient (pcm/K)	-2.8*	-2.8	-
ITC (pcm/K)	-47.9	-46.8	2.3

* - Calculated by CRONOS2

Figure 8.3 presents a comparison of the assembly power distributions calculated by PARCS and BARS at initial conditions.

Comparison of the steady-state results obtained by using different methods, allows to give the following conclusions:

- a good agreement was found for worth of regulating banks and single rods H8 and H12 as well as for the temperature coefficients of reactivity;
- the BARS model overestimated worth of single peripheral rod N12 approximately by 60% (it is important to note that such an overestimation in rod worth may result in the increase in local peak enthalpy increment by a factor of 2 or even more);
- the BARS model overestimate the average peaking factor for an axial power distribution by 17%;
- maximum difference in the assembly power distributions was about 13% for the assemblies adjacent to the radial reflector.

0.921	1.875	1.576	1.598	0.665	0.846	0.386	0.284
0.826	1.713	1.457	1.501	0.624	0.806	0.382	0.291
-10.3	-8.6	-7.6	-6.1	-6.2	-4.7	-1.0	2.5
	1.519	1.723	1.281	1.250	0.613	0.929	0.386
	1.389	1.597	1.211	1.216	0.610	0.969	0.410
	-8.6	-7.3	-5.5	-2.7	-0.5	4.3	6.2
		0.820	1.324	1.100	1.314	1.107	0.400
		0.757	1.272	1.150	1.376	1.191	0.451
		-7.7	-3.9	4.5	4.7	7.6	12.7
			0.676	1.244	1.055	0.790	
			0.654	1.257	1.103	0.871	
			-3.3	1.0	4.5	10.2	
				0.726	1.144	0.536	
				0.725	1.210	0.604	
				0.1	5.8	12.7	
PARCS					0.660		
BARS					0.748		
ε ,%					13.3		

Figure 8.3 Power Distribution at Initial Conditions

Note that the maximum deviation in the assembly power distribution was observed in peripheral assemblies with two facets adjacent to the radial reflector, This fact may be partly explained by different approaches of preparation of the neutron databases for the fuel and reflector regions. In the assembly-by-assembly model, neutron cross sections for fuel assembly are generated under the assumption that this assembly is surrounded by similar assemblies with specified boundary conditions for neutron current at its facets. It is clear, that such a model is not adequate in case when the considered assembly in the core is surrounded also by the reflector region. This disparity will be larger for assemblies surrounded by the reflector from two sides. The pin-by-pin model, as the ZR-6 validation results showed, successfully overcomes such troubles. Nevertheless, this problem deserves comprehensive investigation using precise codes to model LWR core-reflector interface.

It should be paid attention to a significant difference in worth of control rod N12 compared with one of control rod H12. Calculational results show that when one or other control rod is withdrawn, a distortion in the fuel pin power distribution takes place. Withdrawal of the most peripheral rod results in the largest distortion in the power distribution. To characterize a degree of a power distortion Table 8.2 shows radial peaking factors (RPFs) in pin-by-pin power distributions calculated by the BARS code for initial conditions and when one of the rods was withdrawn. The third column of the table contains RPF in power distributions averaged on each assembly.

Table 8.2 Radial Peaking Factors in Pin-by-Pin Power Distribution

Type of calculation	Pin-by-pin RPF	Averaged RPF
Initial conditions (Banks 5-7 in)	1.85	1.71
Withdrawal of rod H8	2.80	2.59
Withdrawal of rod H12	2.55	2.39
Withdrawal of rod N12	6.22	5.07

When a power distribution is rather smooth over the core, the averaged RPF may be considered as analogous to RPF calculated by the assembly-by-assembly model. In this case boundary conditions for neutron current between fuel assemblies are more or less equivalent to those used during generation of cross sections.

But in case of a large power distortion in the local area of the core, the model of generation of assembly average cross sections may be not adequate due to intra-assembly effects. Especially, these effects are displayed for assemblies adjacent to the accident one.

Comparison of RPFs for withdrawal of rods H8 and H12 shows that the power deviations are not so large in these cases. That is why the results from different codes are well agreed (see Table 8.1). On the contrary, in case with withdrawal of rod N12, the pin-by-pin RPF becomes a factor of 3.4 higher compared with the unperturbed case. In the vicinity of assembly N12 (this area included also 4 neighboring assemblies) a very large distortion in pin-by-pin power distribution arose (Figure 8.4). Correct description of such distortion in the framework of the assembly-by-assembly model is problematic. This is a question of principal in REA analysis by the pin-by-pin and the assembly-by-assembly models.

8.2. Intercomparison Between the Pin-by-Pin and Assembly-by-Assembly Models in a PWR REA

It is obvious that observed differences in the steady-state parameters could result in significant uncertainties in REA consequences (especially when the peripheral rod is ejected) and it would be difficult to do reasonable comparison of REA calculations from different methods. For this reason, to provide initial steady-state conditions as close as possible, the radial reflector neutronic model in the BARS code was changed by artificial increase in the neutron absorption by boron poisoning of 1000 ppm. As for axial reflectors, the data for the bottom one were used for both reflectors. After such corrections in the BARS reflector model, the maximum deviation in a power distribution became no more than 6% (Figure 8.5). Table 8.3 gives major steady-state parameters after the correction.

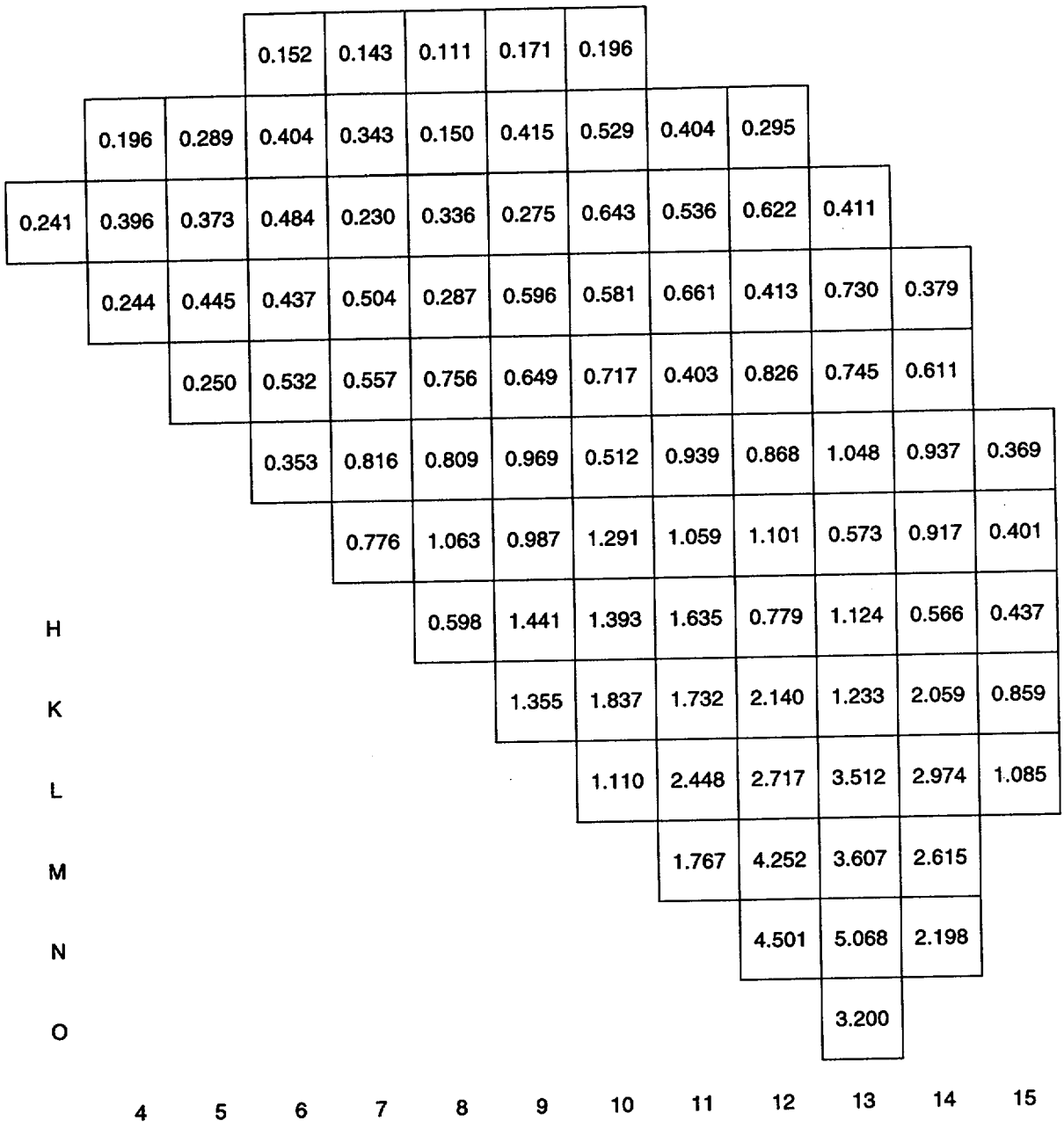

Figure 8.4 Power Distribution After Withdrawal of Rod N12

0.921 0.869 -5.6	1.875 1.790 -4.5	1.576 1.515 -3.9	1.598 1.557 -2.5	0.665 0.647 -2.7	0.846 0.820 -3.1	0.386 0.383 -0.8	0.284 0.274 -3.5
	1.519 1.447 -4.7	1.723 1.662 -3.5	1.281 1.250 -2.4	1.250 1.247 -0.2	0.613 0.618 0.8	0.929 0.961 3.4	0.386 0.390 1.0
		0.820 0.787 -4.0	1.324 1.307 -1.3	1.100 1.165 5.9	1.314 1.371 4.3	1.107 1.162 5.0	0.400 0.411 2.7
			0.676 0.668 -1.2	1.244 1.255 0.9	1.055 1.078 2.2	0.790 0.816 3.3	
				0.726 0.709 -2.3	1.144 1.155 1.0	0.536 0.538 0.4	
					0.660 0.667 1.1		

PARCS BARS ε ,%

Figure 8.5 Power Distribution at Initial Conditions After Reflector Model Correction

Table 8.3 Steady-State Parameters After Reflector Model Correction

Parameter	PARCS	BARS	Deviation (%)
Worth of Bank 5 (pcm)	1423	1532	7.6
Worth of Bank 6 (pcm)	849	856	0.8
Worth of Bank 7 (pcm)	1050	1083	3.1
Worth of rod H8 (pcm)	347	349	0.6
Worth of rod H12 (pcm)	188	204	8.5
Worth of rod N12 (pcm)	344	473	38
Axial peaking factor	2.65	2.68	1.1

As shown from the table, differences in the worth of regulating banks became smaller, but as before the correction the rod N12 worth differs significantly from the PARCS one. Thus, despite all corrections in the reflector model, a large difference in the worth of peripheral rod N12 still exists. The most probable explanation of this phenomenon is intra-assembly effects when a large distortion in the power distribution occurs at a local area of the core near the reflector.

Below the results of REA calculations with different codes are presented. The basic scenario was a fast ejection of the central control rod with fixed worth of 1.2$ (with the delayed neutron fraction of 521 pcm). To provide the last value (instead of 0.67$ in reality) some modifications were done in each code.

BARS and PARCS used the same thermal-hydraulic code (RELAP5) with the similar input decks, while CRONOS2 was coupled with the FLICA4 thermal-hydraulic code.

Table 8.4 presents some parameters of the REA. The agreement is very good between all codes. Local fuel enthalpy reaches its peak value at the same assembly H9 and the same axial node at the top of the core. The maximum increment in fuel enthalpy in assembly H9 was about 19 cal/g (BARS) and 17 cal/g (PARCS).

Table 8.4 Parameters of the REA

Parameter	RELAP-PARCS	RELAP-BARS	FLICA4-CRONOS2
Control rod worth ($)	1.206	1.209	1.196
Peak power (GW)	10.89	10.69	10.37
Time of peak power (ms)	360	338	360
Power pulse width (ms)	65	63	69

Another direction in the intercomparison was to compare the intra-assembly power distribution in the hottest assembly (H9) calculated "directly" by BARS and reconstructed by a special procedure used together with the PARCS code. (Note, that this procedure is used as independent part of calculations and does not influence the calculational routine.) This comparison for the initial time moment and the time when reactor power reaches peak value, is presented in Reference 10. The agreement of the data is rather good. Both methods indicate the same location of the hottest pins (Figure 8.2). Local peaking factors in assembly H9 were 1.27 (BARS) and 1.25 (PARCS) for the initial time moment and 1.08 (BARS) and 1.07 (PARCS) for peak power.

It is important to emphasize that the intercomparison of such a kind for the accident with the peripheral rod ejection could be of the most interest because of more dramatic consequences. Such transient (under the assumption of stuck rod near the accident one) does not require any artificial modification in worth of the ejected rod.

Next part of this REA study concerns intra-assembly representation of fuel temperature during the transient. As before mentioned, two cases for the fuel temperature representation were considered in the REA calculation:

- Case 1 – the assembly-by-assembly model;
- Case 2 – the pin-by-pin model.

8.3. Validation of Fuel Temperature Reconstruction Method

The validation of the reconstruction method for the intra-assembly fuel temperature distribution within any assembly was done directly in the framework of the REA calculation. For this reason a number of fuel pins of interest were considered as separate heat structures in the RELAP input deck. This allowed comparing fuel temperatures in selected fuel pins calculated "directly" by RELAP and by "approximate" reconstruction method.

Figure 8.6 shows fuel temperature increment for the hottest fuel pellet calculated "directly" (solid curve) and relative deviation between "approximate" and "direct" calculations (dashed curve) as a function of the time of the accident. As it was shown in the figure, the relative uncertainty of the reconstruction method for the hottest fuel pin compared with "direct" calculation did not exceed 1.5% during the transient (this resulted in the temperature deviation of no more than 1.5 K at the time of the peak power).

Thus, the following conclusion can be done: the reconstruction method allows to calculate the fuel temperature distribution within any assembly during a REA with a reasonable accuracy.

8.4. Effect of Detailed Intra-Assembly Fuel Temperature Representation

Figures 8.7 and 8.8 show reactor power and enthalpy increment for the hottest fuel pellet as functions of the time of the transient. These dependencies are given as solid curves calculated for Case 2. Here the relative deviations between Case 2 and Case 1 are indicated as dashed curves. As the figures show, the relative difference in calculations of the reactor power and the fuel enthalpy by two methods did not exceed 2.5% with decreasing to 1% at the end of the transient.

Table 8.5 presents major parameters of the transient calculated by both models. The last column gives relative deviation between Case 2 and Case 1.

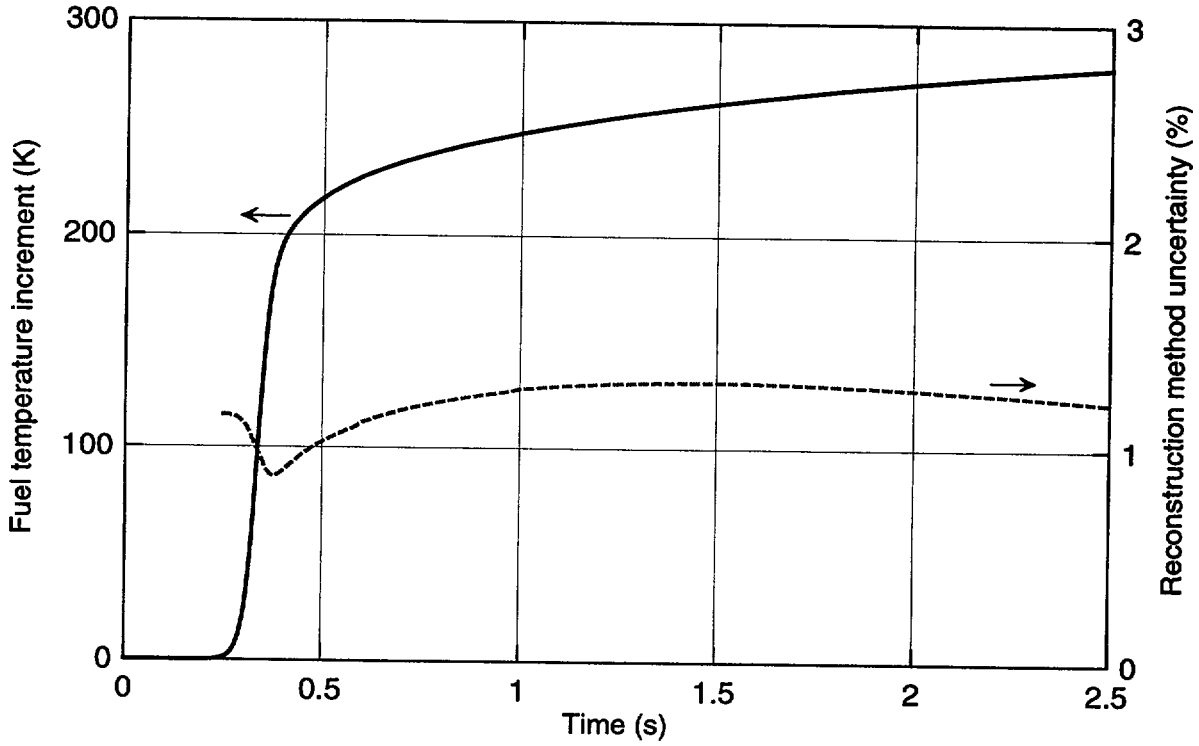

Figure 8.6 Fuel Temperature Increment in the Hottest Fuel Pellet vs. Time

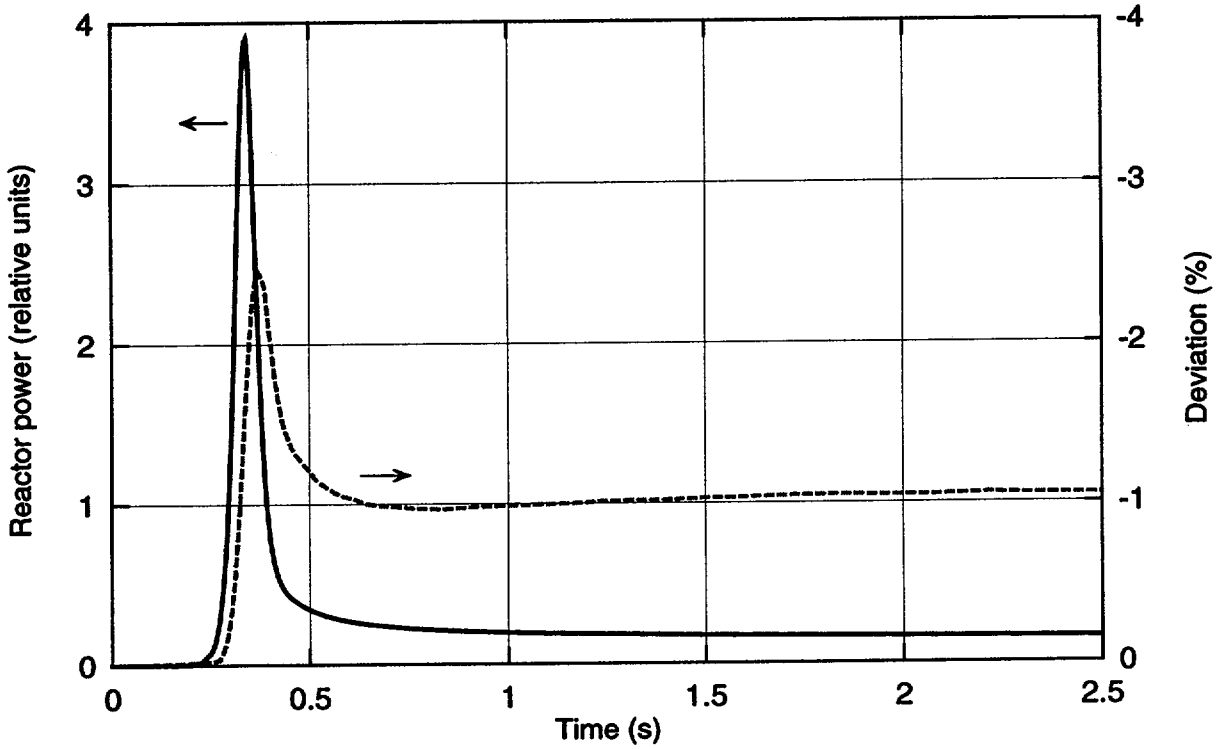

Figure 8.7 Reactor Power vs. Time

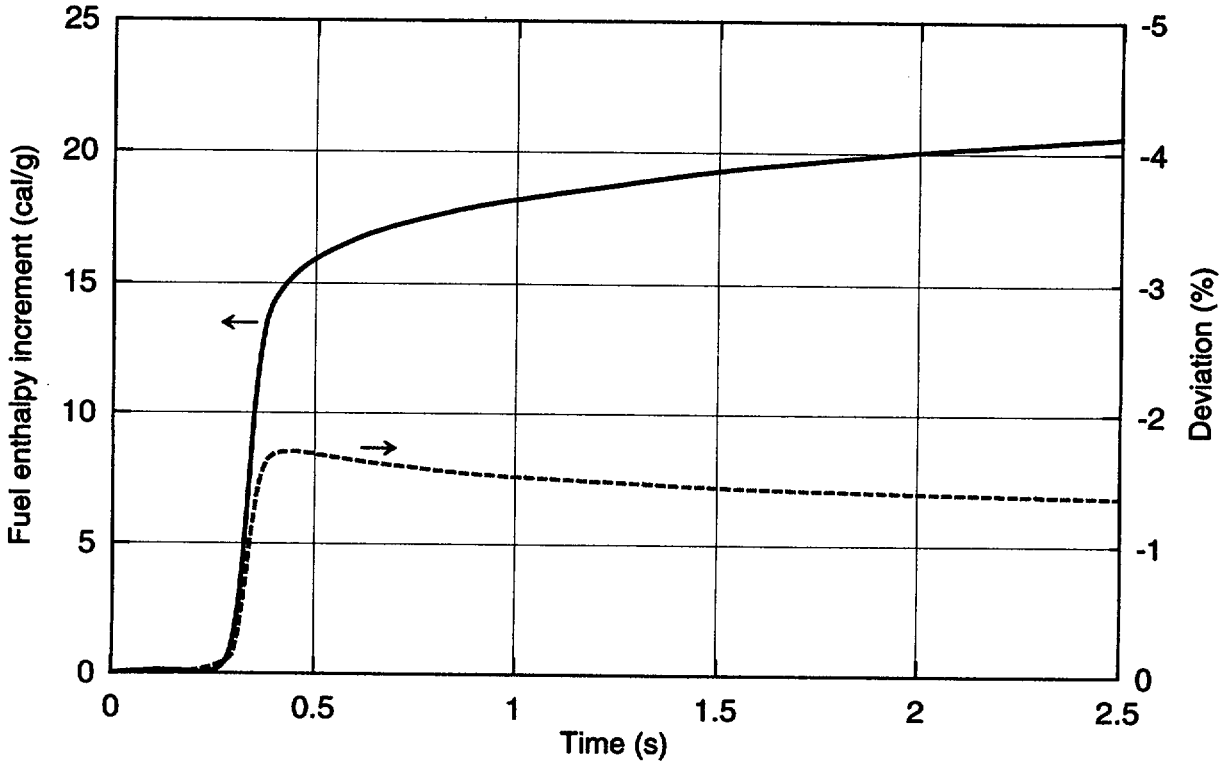

Figure 8.8 Enthalpy Increment for the Hottest Fuel Pellet vs. Time

As the Figure 8.7 shows, the reactor power reached the peak value at 0.34 s when the maximum increase in fuel temperature for the hottest assembly was about 100 K (see Figure 8.6). At the same time the maximum difference in fuel temperature across this assembly was less than 10 K. Such relatively low fuel temperature non-uniformity and not great fuel temperature increment during the transient were key factors which allow to understand why all parameters calculated in both cases are well agreed.

Table 8.5 Main Parameters of the REA with Different Fuel Temperature Models

Parameter of transient	Case 1	Case 2	Deviation
Peak power of the core (GW)	10.69	10.51	-1.7%
Peak power of the fuel pin (kW)	835	821	-1.7%
Maximum temperature in fuel pin (K)	834.6	834.5	-0.1K
Maximum increment in fuel enthalpy (cal/g)	20.6	20.3	-1.4%

Comparison of the results shown that calculation with assembly-by-assembly fuel temperature representation gave slightly conservative results in key parameters of the transients in the comparison with the pin-by-pin one.

9. CONCLUSIONS

The major goal of this study was to analyze effects of the pin-by-pin representation of fuel power, burnup and temperature on the course of LWR RIAs. The pin-by-pin model, based on the heterogeneous reactor theory, was implemented in the BARS code. A coupling of BARS with RELAP5/MOD3 and some interface codes allow by now to solve a wide range of problems of interest for various types of reactors:

- steady states at different conditions (including determination of reactivity effects);
- slow transients (including modeling of LWR fuel cycle);
- fast transients (including LWR RIAs such as control rod ejection and steam line break).

Unlike nodal diffusion models used the assembly-by-assembly approach, the pin-by-pin model opens qualitatively different opportunities in the analysis of the intra-assembly effects of fuel power, burnup and temperature on consequences of LWR RIAs.

Validation results obtained for critical assembly ZR-6, demonstrate capabilities of the BARS code to predict fine pin-by-pin power effects near fuel-reflector boundary and in the vicinity of any perturbation in the core. Similar effects in the pin-by-pin power distribution were found in the RELAP-BARS modeling of the peripheral control rod ejection in VVER-1000 of the South Ukrainian NPP Unit 1 with core burnup of about 21 MWd/kgU. The REA analysis showed that:

- ejection of a peripheral control rod resulted in very complicated pin-by-pin power distribution in assemblies directly adjacent to the accident one;
- fuel assemblies with relatively low power contained fuel rods with power exceeded maximum value for fuel rods in assembly with peak power;
- the hottest fuel rod did not necessarily belong to assembly with peak power; for this reason an assembly-by-assembly model may result in underestimation of the local peak enthalpy, because of a flux reconstruction method is used, as a rule, only for the assembly with peak power.

Effects of the pin-by-pin burnup representation compared with the assembly-averaged model were found as rather small for such slightly burnt-out cores.

Intercomparison of calculational results for TMI-1 obtained with different neutronic models: the pin-by-pin one (BARS) and the assembly-by-assembly (PARCS and CRONOS2), displayed a number of problems which are very important in reactor safety analysis. There were noticeable differences in the radial and axial power distributions. Besides, the BARS value for the worth of single peripheral control rod was approximately 60% higher. This fact can play a major role in safety analysis of such a REA. A supposition about significant influence of a large power distortion (intra-assembly effect) in a local area of the core on neutronic parameters was put forward.

On the contrary, worths of the regulating banks and central control rod were in a rather good agreement. Comparison of the calculational results for the accident with ejection of the central control rod with fixed worth of 1.2$ and adjusted reflector model in the BARS code, show also a very good agreement between different codes. Besides, in this case the procedure of neutron flux reconstruction used together with PARCS gives quite satisfactory results for the pin-by-pin restoration of the power distribution within the assembly adjacent to the accident one.

Another intra-assembly effect considered in this study was the effect of the pin-by-pin fuel temperature representation. As the RELAP-BARS calculations of the TMI-1 REA shows this effect is rather small. The calculation using assembly-by-assembly fuel temperature distribution gave slightly conservative results in key parameters of the REA.

Summarizing the results of this study, the following general conclusion may be submitted. No doubt, intra-assembly effects play significant role in prediction of many important parameters of reactor safety such as worth of ejected control rod and local fuel enthalpy. It is evident that comprehensive analysis of the RIA with a large distortion of the power distribution demands to use the pin-by-pin model.

In the future work, main efforts should be applied to further calculational investigations of the problems, which were pointed out in this report, namely:

- validation of the fuel cycle model for long duration cycles in VVER and PWR with cores containing burnable absorbers;
- analysis of effects of burnup representation for REA in a VVER with high burnup core;
- study of effects of the LWR fuel-reflector interface and worth of control rods on the basic safety parameters by comparison with precise codes;
- analysis of above mentioned effects for the accident with the peripheral control rod ejection or other RIA, such as, for example, boron dilution accident in a VVER or a PWR.

10. REFERENCES

1. D. Diamond and L. Neymotin, "Sensitivity Studies for the BWR Rod Drop Accident," Letter Report FIN W6382, October 31, 1996.
2. "RELAP5/MOD3.2 Code Manual," NUREG/CR-5535, INEL-95/0174, 1995.
3. A. Avvakumov and V. Malofeev, "Three-Dimensional Simulation of Delayed Neutron Transients in a Heterogeneous Reactor," *At. Energy*, 70 (1), 1991.
4. A. Avvakumov and V. Malofeev, "An Advanced 3 D Pin-by-Pin Neutronic Model for the LWR RIA Analysis: Features, Advantages and Validation," Report No. 90-12/1-8-97, Nuclear Safety Institute of Russian Research Centre "Kurchatov Institute", 1997.
5. A. Avvakumov, et al., "Validation of the BARS Code Package with ENDF/B Based Data Library," Report No. 90-12/1-4-98, Nuclear Safety Institute of Russian Research Centre "Kurchatov Institute", 1998.
6. A. Avvakumov and V. Malofeev, "Validation of an Advanced Heterogeneous Model for LWR Detailed Pin-by-Pin Calculations," Proceedings of the International Conference on the Physics of Nuclear Science and Technology, Long Island, NY, October 1998.
7. A. Avvakumov and V. Malofeev, "Validation of a Pin-by-Pin Neutron Kinetics Method for LWRs," Proceedings of the International Twenty-Sixth Water Reactor Safety Information Meeting, Bethesda, Maryland, October 1998.
8. H.G. Joo, et al., "PARCS: A Multi-Dimensional Two-Group Reactor Kinetics Code Based on the Nonlinear Analytic Nodal Method," PU/NE-98-26, Purdue University, September 1998.
9. J.J. Lautard, S. Loubiere, C. Fedon-Magnaud, "CRONOS, A Modular Computational System for Neutronic Core Calculations,"Proc. IAEA Specialist Mtg. on Advanced Calculational Methods for Power Reactors, Cadarache, France, September 1990.

10. D.J. Diamond, et al., "Intercomparison of Results for a PWR Rod Ejection Accident," Proceedings of the International Twenty-Seventh Water Reactor Safety Information Meeting, Bethesda, Maryland, October 1999.

11. A. Kwaratzhely and B. Kochurov, "A Method for Calculation of Neutronic Parameters in a Heterogeneous Reactor Cell," *At. Energy*, 58 (2), 1985.

12. B. Kochurov and V. Malofeev, "A Difference Approach to the Solution of Heterogeneous Reactor Equations," *Annals of Nuclear Energy*, 4, 21, 1977.

13. B. Kochurov, "Effective Resonance Levels," *At. Energy*, 60 (3), 1986.

14. R.E. McFarlane, "NJOY91.91: A Code System for Producing Pointwise and Multigroup Neutron and Photon Cross Sections from ENDF/B Evaluated Nuclear Data," ORNL PSR-171, Oak Ridge National Laboratory, 1993.

15. "ENDF/B Summary Documentation," BNL-NCS-17541 (ENDF-201), 4th ed. (ENDF/B-VI), P. F. Rose, Ed., Brookhaven National Laboratory (Oct. 1991; Release-2, 1993; Release-3, 1996).

16. V. Davidenko and V. Tsybulsky, "Detailed Calculation of Neutron Spectrum in a Cell of a Nuclear Reactor," Proceedings of the International Conference on the Physics of Nuclear Science and Technology, Long Island, NY, October 1998.

17. R.D. Mosteller, et al., "Benchmark Calculations for the Doppler Coefficient of Reactivity," *Nuclear Science and Engineering*, 107, 265, 1991.

18. F. Rahnema and H.N.M. Gheorghiu, "ENDF/B-VI Benchmark Calculations for the Doppler Coefficient of Reactivity," *Annals of Nuclear Energy*, 23, 12, 1996.

19. F. Rahnema, D. Ilas, and S. Sitaraman, "Boiling Water Reactor Benchmark Calculations," Nuclear Technology, 117, 184, 1997.

20. "Experimental Investigations of the Physical Properties of VVER-type Uranium-Water Lattices," Final Report of TIC, Budapest, Akademiai Kiado, 1 (1985), 3 (1991).

21. "The VVER Experiments: Regular and Perturbed Hexagonal Lattices of Low-Enriched UO_2 Fuel Rods in Light Water," Report LEU-COMP-THERM-015, vol. IV, KFKI, Budapest, 1996.

22. S.P. Szabo and R.J. Stammler, "HELIOS: Benchmarking Against Hexagonal TIC Experiments," Proceedings of the International Conference on the Physics of Nuclear Science and Technology, Long Island, NY, October 1998.

23. A.D. Galanin, "Revision of Scheme for the Major Fission Products with Weak Effective Fission Product," Preprint ITEP-135, 1989 (Rus).

24. L. Markova, "CB2 Result Evaluation (VVER-440 Burnup Credit Benchmark)," 9th AER Symposium on VVER Reactor Physics and Reactor Safety, Slovakia, October 4-8, 1999.

25. "Post-Irradiation Examinations of Fuel Assembly No. 4436001114 Irradiated at NV NPP Unit 5 During 3 Fuel Cycles up to Burnup of 44.7 MWd/kgU," O-4011, RIAR, Dimitrovgrad, 1991 (Rus).

26. "Post-Irradiation Examinations of Fuel Assemblies Nos. 14422198 and 14422222 Irradiated at Kola NPP Unit 3 up to Burnups of 46.22 and 48.18 MWd/kgU," O-4326, RIAR, Dimitrovgrad, 1994 (Rus).

27. "In-Core Fuel Management Code Package Validation for WWERs," IAEA-TECDOC-847, November, 1995.

28. A. Avvakumov, et al., "3 D Pin-by-Pin Modeling of Rod Ejection RIA in VVER-1000," Report No. 90-12/1-33-97, Nuclear Safety Institute of Russian Research Centre "Kurchatov Institute", 1997.

29. K.N. Ivanov et al., "Pressurized water Reactor Main Steam Line Break (MSLB) Benchmark; Volume I: Final Specifications," NEA/NSC/DOC(99)8, U.S. Nuclear Regulatory Commission and OECD Nuclear Energy Agency, April 1999.

NRC FORM 335 (2-89) NRCM 1102, 3201, 3202

U.S. NUCLEAR REGULATORY COMMISSION

BIBLIOGRAPHIC DATA SHEET

(See instructions on the reverse)

1. REPORT NUMBER (Assigned by NRC, Add Vol., Supp., Rev., and Addendum Numbers, if any.)
NUREG/IA-0175
NSI RRC K190-12/1-3-00
IPSN/00-13

2. TITLE AND SUBTITLE
Analysis of Pin-by-Pin Effects for LWR Rod Ejection Accident

3. DATE REPORT PUBLISHED
MONTH: February
YEAR: 2000

4. FIN OR GRANT NUMBER
W6500

5. AUTHOR(S)
A. Avvakumov, V. Malofeev, V. Sidorov

6. TYPE OF REPORT
Technical

7. PERIOD COVERED *(Inclusive Dates)*

8. PERFORMING ORGANIZATION - NAME AND ADDRESS *(If NRC, provide Division, Office or Region, U.S. Nuclear Regulatory Commission, and mailing address; if contractor, provide name and mailing address.)*
Nuclear Safety Institute of Russian Research Centre
"Kurchatov Institute"
Moscow, Russia

9. SPONSORING ORGANIZATION - NAME AND ADDRESS *(If NRC, type "Same as above"; if contractor, provide NRC Division, Office or Region, U.S. Nuclear Regulatory Commission, and mailing address.)*
Division of Systems Analysis and Regulatory Effectiveness
Office of Nuclear Regulatory Research
U.S. Nuclear Regulatory Commission
Washington, DC 20555-0001

10. SUPPLEMENTARY NOTES

11. ABSTRACT *(200 words or less)*

This study was undertaken to demonstrate the capabilities of the pin-by-pin model used by the BARS code and to understand the various effects of intra-assembly pin-by-pin representation of fuel power, burnup and temperature in calculational analysis of light water reactor rod ejection accidents (LWR REAs). Effects of pin-by-pin fuel power and burnup representation were investigated on the basis of calculations for the peripheral control rod ejection in a VVER-1000 of the South Ukrainian NPP Unit 1. Comparative analysis of the REA in the Three Mile Island pressurized water reactor using the BARS code with the diffusion nodal codes PARCS and CRONOS2 was undertaken. Important differences between the three kinetics codes and the effects of the pin-by-pin fuel temperature representation are discussed.

12. KEY WORDS/DESCRIPTORS *(List words or phrases that will assist researchers in locating the report.)*
BARS, PARCS, CRONOS2, transient analysis, safety analysis, 3D kinetics, coupled thermal-hyrdualic-neutronic computer codes, fuel pin power

13. AVAILABILITY STATEMENT
unlimited

14. SECURITY CLASSIFICATION
(This Page)
unclassified
(This Report)
unclassified

15. NUMBER OF PAGES

16. PRICE

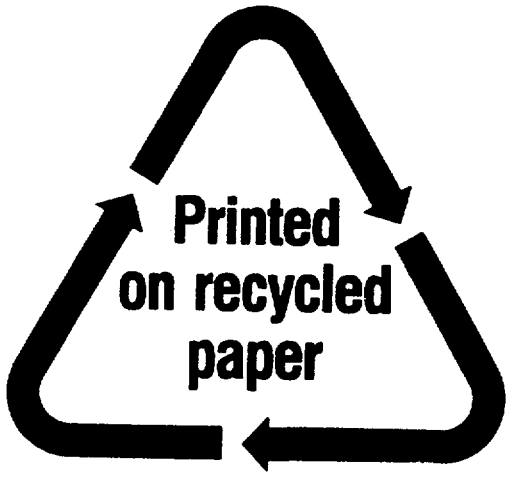

Federal Recycling Program

UNITED STATES
NUCLEAR REGULATORY COMMISSION
WASHINGTON, D.C. 20555-0001